

A STUDY OF DIFFERENT ULTRASONIC STROBOSCOPES  
AND THEIR USEFULNESS FOR THE STUDY OF WAVE  
PROPAGATION AND ACOUSTIC BIREFRINGENCE

by

Walter L. Gessert

AN ABSTRACT

Submitted to the School of Graduate Studies of Michigan  
State College of Agriculture and Applied Science  
in partial fulfillment of the requirements  
for the degree of

DOCTOR OF PHILOSOPHY

Department of Physics and Astronomy

1954

Approved E. A. Hieplemann

Walter L. Gessert

ABSTRACT

The need for a stroboscope suitable for the study of acoustic birefringence in particular portions of a sound wave is stated, and the present situation of acoustic birefringence theories is given in summary. The theory for use of two sound waves for stroboscopic effects is discussed (1), and the results of experimental examination of some of these effects are shown, especially where a first sound wave is situated at a secondary light source. Simple pictures of some geometrical demonstrations are shown.

The Rayleigh (2) phase shift by reflection of sound at a liquid-liquid interface is studied showing good agreement with theory.

The phase relationship in the field in the near-neighborhood of a long, narrow "piston-like" quartz transducer (3) is examined and shows that the apparent cylindrical waves from the edges of the quartz are out of phase with the plane waves by one-half wavelength. The phase change at the focus for a cylindrical wave (4) is mentioned and data given which is not in agreement with theoretical conclusions. A conclusion is written for the use of Bär's stroboscope.

1. R. Bär, *Helv. Phys. Acta* (8), 9, 654,678 (1936).
2. Lord Rayleigh, *The Theory of Sound*, Second Edition, Macmillan (1896), Vol. II, PP. 84 (Reprinted 1929).
3. K. Osterhammel, *Akust. Zeits.*, 6, 6 (1941).
4. F. Reiche, *Ann. d. Phys.*(4), 29, 65 (1909).

A STUDY OF DIFFERENT ULTRASONIC STROBOSCOPES  
AND THEIR USEFULNESS FOR THE STUDY OF WAVE  
PROPAGATION AND ACOUSTIC BIREFRINGENCE

BY

Walter L. Gessert

A THESIS

Submitted to the School of Graduate Studies of Michigan  
State College of Agriculture and Applied Science  
in partial fulfillment of the requirements  
for the degree of

DOCTOR OF PHILOSOPHY

Department of Physics and Astronomy

1954

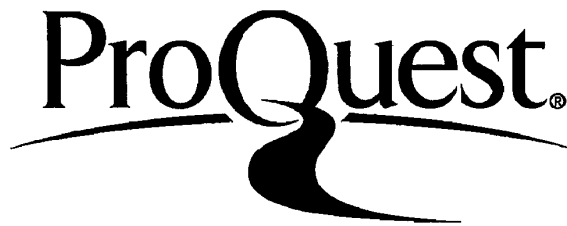
ProQuest Number: 10008462

All rights reserved

INFORMATION TO ALL USERS

The quality of this reproduction is dependent upon the quality of the copy submitted.

In the unlikely event that the author did not send a complete manuscript and there are missing pages, these will be noted. Also, if material had to be removed, a note will indicate the deletion.



ProQuest 10008462

Published by ProQuest LLC (2016). Copyright of the Dissertation is held by the Author.

All rights reserved.

This work is protected against unauthorized copying under Title 17, United States Code  
Microform Edition © ProQuest LLC.

ProQuest LLC.  
789 East Eisenhower Parkway  
P.O. Box 1346  
Ann Arbor, MI 48106 - 1346

#### ACKNOWLEDGEMENTS

The author wishes to take this opportunity to express his sincere gratitude to Dr. E. A. Hiedemann for suggesting the problems in acoustic birefringence and for his continuing interest and guidance in the results which have been achieved. Thanks are also due to Drs. R. D. Spence and F. Leitner for discussions on portions of the work on the diffraction field and to Mr. M. A. Breazeale for the great assistance in the photographic work and in the adjustment of the optical equipment. Especially, the author acknowledges the financial assistance given under a U. S. Army Ordnance Contract without which the work could not have been accomplished.

## TABLE OF CONTENTS

	Page
INTRODUCTION	
Acoustic Birefringence	1
Ultrasonic Stroboscopy	6
THEORY	
Use of Two Sound Waves	9
Phase Shift upon Reflection at a Liquid-Liquid Interface	13
Diffraction Wavefield before a Beam Forming Quartz	16
Phase Change at the Focus of a Cylindrical Lens	20
EXPERIMENTAL APPARATUS	
Oscillator and Power Supply	21
Optical Equipment	25
Ultrasonic Equipment	25
DISCUSSION	
Comparison of Two Velocities	26
Tank <sub>1</sub> in Divergent Light	33
Bar Stroboscope: T <sub>1</sub> at D'	37
Raleigh Phase Shift	46
Diffraction Field before a Beam-Forming Quartz	51
Phase Change at the Focus of a Cylindrical Lens	54
GENERAL CONCLUSIONS	58
BIBLIOGRAPHY	59

## LIST OF FIGURES

Figure	Page
1. Light Intensity Versus Square of Transducer Current.	5
2. Optical Arrangement.	9
3. Tank $T_1$ in Divergent Light.	11
4. Interference Points from Incident and Reflected Sound Beams.	14
5. Measurement of $D$ and $d$ .	15
6. Drawing of Interference Points for Plane and Cylindrical Waves in Phase.	17
7. Drawing of Interference Points for Plane and Cylindrical Waves out of Phase by $180^\circ$ .	18
8. Phase Change in the Region of the Focus for Spherical Waves (Reiche).	20
9. Circuit of Oscillator and Amplifiers.	22
10. Circuits of Power Supplies.	23
11. Impedance Matching Circuit.	24
12. Theoretical Curves for Velocity Comparison.	28
13. Photographs of Fringes for Calculating Velocity Differences.	29
14. Relationship between $\lambda_1$ and $\lambda'_1$ .	33
15. Experimental Curve for $d$ vs $\lambda$ .	35
16. Revised Optical Arrangement by Bär.	38
17. Broadening of Slit Image.	38
18. Photographs of Interference Points.	42
19. Sound Waves Focused by Cylindrical Plastic Lens.	43
20. Sound Diffraction Grating.	44
21. Diffraction Orders Brought to Focus by Lens.	45

Figure	Page
22. Experimental Curve for $\theta_1$ vs $2\epsilon$ .	47
23. Evidence of Rayleigh Waves in Mica Film.	50
24. Enlarged Image of the Neighborhood of a Long Thin Quartz.	52
25. Sound Waves Brought to a Focus by Cylindrical Lens.	55



## INTRODUCTION

It is not unusual for the thesis work to have been initiated with one purpose in view only to be changed, or narrowed down, to a purpose quite different from the original. The present work had as a main objective the experimental examination of the theoretical predictions of three different theories for accidental acoustic birefringence. In the course of experiments to this end it was deemed necessary for reasons to be given below to use a stroboscope especially suited for this study.

A form of stroboscope briefly mentioned by Bär (1) suggested itself as a likely method because of its promise of better light intensity than other stroboscopes furnish; but unfortunately Bär was unable to publish a critical discussion of the effectiveness of his stroboscope due to his untimely demise.

Once work had been started on the method it was decided to limit the purpose of this thesis to an evaluation of the method and to its use upon a number of problems for which it is well suited.

In the course of the initial work upon the matter of birefringence in liquids a fair amount of experimental work had been completed; this work will be briefly summarized.

### Acoustic Birefringence

The fundamental relationship for dynamic (flow) birefringence ( $\Delta n$ ) is that given by Maxwell (2):

$$\Delta n = n_e - n_o = M \eta \frac{\partial u}{\partial z} \quad (1)$$

where  $n$  is refractive index,  $M$  is Maxwell's constant,  $\eta$  is the common shear viscosity and  $u$  is the x-component of velocity; and  $\partial u / \partial z$  is the velocity gradient perpendicular to the flow which is in the x direction. This relationship for flow is used by analogy in two of the three present day theories for acoustic double-refraction.

Stress Birefringence Theory of Lucas (3)(4)(5). This gives a macroscopic picture of an acoustic birefringence due to elastic deformation in the liquid associated with a plane progressive wave. Lucas began with the Navier-Stokes equations for viscous liquids, obtained a velocity gradient from a wave equation for displacement, and arrived at the following:

$$\Delta n = \eta M \frac{\omega}{V} \sqrt{\frac{2I}{\rho V}}, \quad (2)$$

in which  $\omega$  is the circular frequency,  $I$  is sound intensity,  $\rho$  is the density, and  $V$  is the sound velocity.

The Peterlin Theory. Peterlin (6) further developed the successful treatment of Peterlin-Stuart (7) for flow birefringence into a microscopic, orientation theory which postulates the kinematical effect upon asymmetrical particles of any nature in the fluid. The optically anisotropic particles are oriented by the velocity gradient and tend to rotate with an irregular, but periodic motion, passing most slowly through the position in which the major axis is aligned with the direction of flow. The velocity gradient in this case is parallel to the flow. The final result given by Peterlin is:

$$\Delta n = n \eta \frac{\omega}{V} M \sqrt{\frac{2I}{\rho V}}, \quad (3)$$

an expression quite similar to that of Lucas.

Oka Particle-Orientation. This is a second microscopic theory of acoustical double refraction. It is due to Oka (8)(9) who based the orientation of optically anisotropic particles, and therefore the double refraction obtained upon the sound pressure. Here, as in the Peterlin theory, a colloidal suspension is intended. Symmetrical particles which do not partake entirely of the motion of the suspending medium behave in a sound field like freely suspended Rayleigh disks. Depending upon whether they are more or less dense than the suspending medium they experience a torque tending to align them perpendicular or parallel to the direction of sound propagation (10). Oka makes use of an ideal special case which has been calculated by King (11), who assumed perfectly stiff, infinitely thin disks having a radius much smaller than the wave length of the sound. The resulting distribution functions and net birefringence equation for the system are lengthy, but the characteristics can be given briefly. The double refraction ( $\Delta n$ ) is an inverse function of temperature, no frequency dependence is indicated, and when the acoustic intensity ( $I$ ) is small, the double refraction is proportional to  $I$ .

From a cursory examination of the Lucas and the Peterlin results it can be shown that both predict a light transmission through crossed nicol prisms which is proportional to sound intensity, whereas the King-Oka theory predicts transmission proportional to square of the sound intensity. The first two theories are given for plane-progressive waves while the Oka theory is set up for standing waves.

Zvetkov, Mindlina and Makarov (12) working in certain vegetable oils found the birefringence ( $\Delta n$ ) to be proportional to sound amplitude in agreement with the Lucas and Peterlin work. Bennett and Hall (13) also found this to be true for poly-alpha-methyl styrene, a Dow Chemical

Company Resin 276-V2 which is "primarily" composed of tri-polymer alpha-methyl-styrene.

In our laboratories an American Instrument Company photometer was used to obtain data for the curve for Castor Oil given in Figure 1. This curve shows that the light intensity through crossed nicols placed at  $45^{\circ}$  with the wave fronts of the sound is proportional to the square of the transducer current, and therefore proportional to the sound intensity (14). Hall (15) obtained a similar curve for poly-alpha-methylstyrene using the same equipment.

Examination of such well defined liquids as the lower alcohols, nitrobenzene, cinnamic aldehyde, and B-phenylethyl alcohol which are reported to be highly birefringent by Sadron (16) in dynamic double-refraction experiments produced no acoustic birefringence. This disagrees with the prediction of Lucas stress theory.

Peterlin and Stuart (17) state in a footnote, page 103;

"Only the measurement of the amount and sign of the birefringence can lead to a binding decision between the previous theories for molecular solutions."

For this reason it was necessary to find an effective stroboscope which would permit the examination of the wave-field itself. In general the birefringence effects are weak so that the stroboscope must permit as much light as possible to pass through the polarizing prisms and liquid. The Lucas-Peterlin theories predict a change in the sign of the double refraction, while the King-Oka theory predicts only a change in the amount.

The Kerr cell was considered but was discarded because of the serious disadvantages listed by Goudet (18):

1. A stable high voltage field is required.

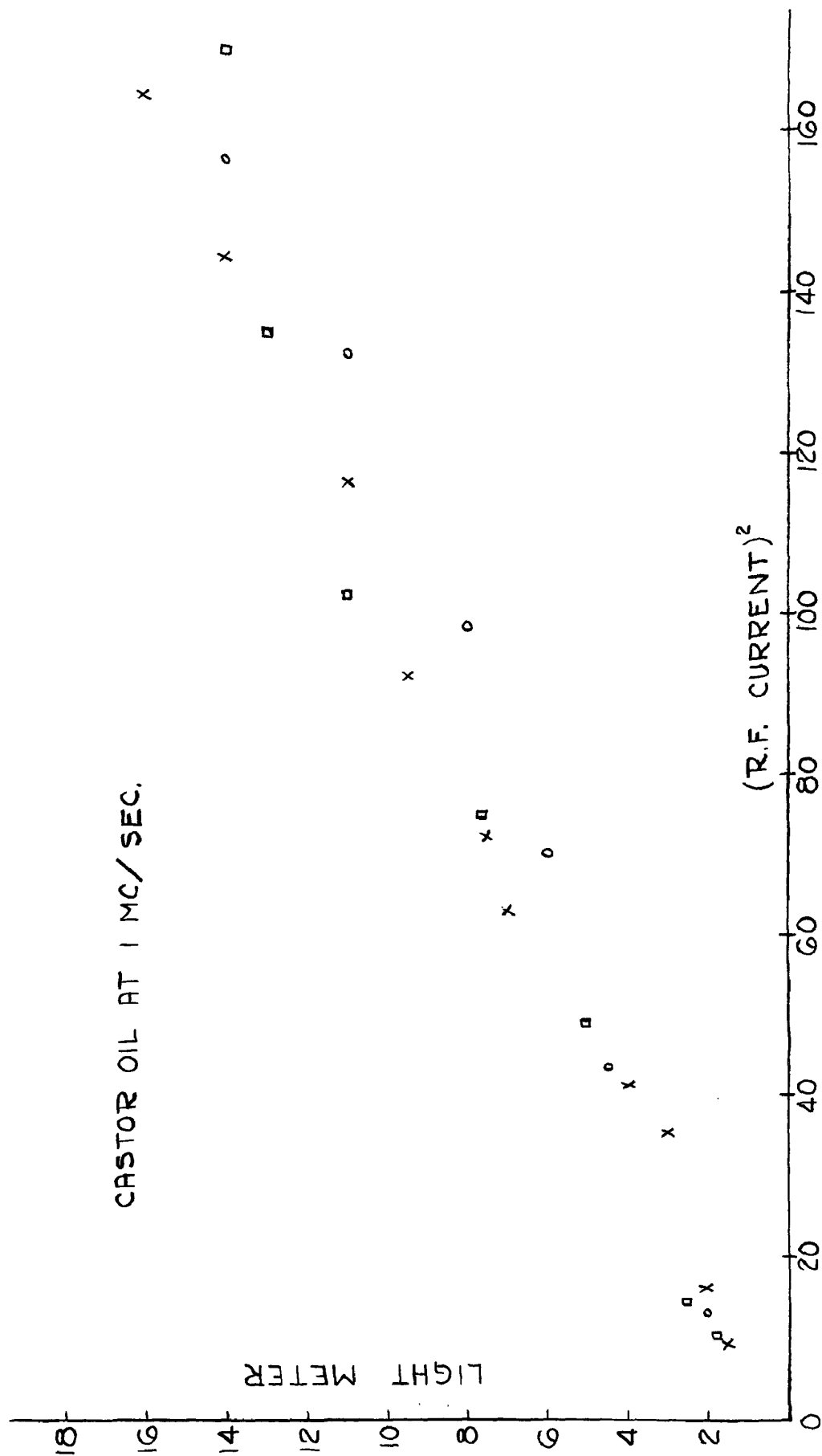


FIGURE 1 LIGHT INTENSITY VERSUS SQUARE OF TRANSDUCER CURRENT

2. The materials with the best Kerr constants are noxious, highly inflammable, or explosive.
3. Thermal conductivity in the liquids is large causing variation of light intensity.

### Ultrasonic Stroboscopy

The different ultrasonic stroboscopes may be listed in three separate classes. The first class obtains its effect from the artificial birefringence (19) which results when certain photo-elastic materials are strained by sound waves. The second uses the modulation of light (20) (21) (22) in the diffraction pattern which is produced when light is passed through an ultrasonic wave-field. The third class is that given by Bär (1) which makes use of the modulation of a light beam by an ultrasonic wave directly as a stroboscopic source for a second ultrasonic beam. From evidence in the literature and from Bär's description of the few trials made by him, there was the promise of a stroboscope which would give a significantly greater light intensity than that obtainable from the first two classes.

Accidental birefringence. The acoustic waves in a quartz of glass block (23) (24) (25) produce an artificial birefringence; when one of these photo-elastic blocks is placed between crossed nicols a beam of light is permitted to pass each half-cycle because of the rotation of the plane of polarization of light in the block and the frequency of illumination is twice the frequency of the exciting oscillator. By proper orientation of the axes of the nicols, one may use the birefringence produced by either the longitudinal waves, transverse waves, or by both (25) (26).

Diffraction pattern. The second class of ultrasonic stroboscopes makes use of the fact that light passing perpendicularly through a stand-

ing or a progressive sound wave is diffracted, or scattered, in a manner similar to that of an ordinary optical grating (20) (21). For a progressive wave the grating moves along with a velocity equal to that of the sound and the grating is present as long as the sound flows through the light. However, when a standing wave is present, the outgoing and reflected sound waves reinforce one another twice during each period so that the grating appears and disappears at a rate equal to twice the sound frequency. Thus the diffraction pattern is modulated at  $2\nu$ , if  $\nu$  is the generator frequency.

The duration of the light in the higher diffraction orders is less than that in the lower orders; also, Hiedemann and Hoesch (25) (26) show that for very intense sound the duration of light in the zero order becomes extremely small, the sound grating being effective during most of the period. Naturally, the use of the light entering the higher orders precludes any thought of a high intensity source since a greater portion of the light is excluded.

The usual ultrasonic fluorometer (27) (28) makes use of this type of light modulation with the further provision that the light incident on a slit placed at one of the diffraction orders is permitted to pass through an optical system of variable path length. The light is brought back through the slit and ultrasonic cell. If the path length is such that the light pulse returns to the sound cell during that portion of a period when the sound grating is not present a minimum is obtained. Thus a 5 mc/sec standing wave modulates the light into pulses of period  $2 \times 10^{-7}$  sec, and the variation of the optical path length further divides this time such that durations of fluorescence of  $10^{-10}$  sec were accurately measured by Rau (29).

Modulation of light by a sound beam. A number of authors (1) (30) (31) (32) (33) have used the modulation of a beam of light directly by a first sound wave. When this light beam passes through a second wave field, the final result depends upon the total action of both sound fields. Tawil (30) first photographed a sound wave in air by having a light beam pass twice through the same sound field before entering a camera focused on the sound field.



## THEORY

### The Use of Two Sound Waves

The effects upon a light beam, which are the result of a passage through two sound fields, are best understood by referring to the schematic drawing shown in Figure 2.

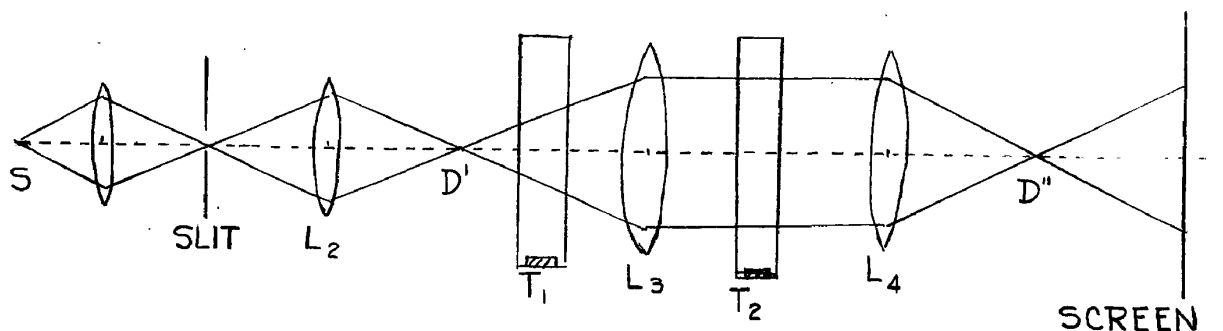


Figure 2. Optical Arrangement.

A source slit (D), or circular aperture, is illuminated by focusing upon it an image of the source S. Lens  $L_2$  forms a secondary source at  $D'$ ; the light from  $D'$  then is collimated by lens  $L_3$  for passage through a glass tank  $T_2$ . Lens  $L_4$  produces an image of  $D'$  at  $D''$ , and, if the distances are proper, there will be formed on the screen an image of the wave-field in  $T_2$ .

Another tank  $T_1$ , may be placed either in the space between  $L_3$  and  $L_4$  together with  $T_2$ , or it may be placed in the space between  $D'$  and the lens  $L_3$ . The case where  $T_1$  is at  $D'$  turns out to be of special interest.

When both tanks are placed in the parallel light in the space between  $L_3$  and  $L_4$  and the quartzs are adjusted so that the two sound beams are antiparallel and perpendicular to the light beam, the assumption is made that the intensity distribution of the light  $i(x,t)$  after passage

through the first beam of progressive sound waves is:

$$i_1(x, t) = 1 - \sin 2\pi \left( \frac{x}{\lambda} - \frac{t}{\tau} \right), \quad (4)$$

where  $x$  is measured parallel to the sound,  $\lambda$  is the wavelength of the sound in the liquid,  $t$  is time, and  $\tau$  is the period.

In similar fashion for the light intensity after passage through the second sound beam:

$$i_2(x, t) = 1 - \sin 2\pi \left( \frac{x}{\lambda} + \frac{t}{\tau} \right), \quad (5)$$

and the observed intensity distribution  $I(x)$  after passage through both sound beams becomes:

$$I(x) = \int_0^\tau i_1 i_2 dt = \tau \left( 1 - \frac{1}{2} \cos 2\pi \frac{x}{\lambda/2} \right). \quad (6)$$

This is in agreement with experimental evidence and one obtains the periodic intensity distribution which is characteristic of a standing wave in one tank wherein the distance between adjacent maxima is equal to a half-wavelength  $\lambda/2$ .

For parallel positioning of the sound beams no lines appear when both tanks contain the same liquid, i.e. the wavelengths of the sound in each tank are equal. But when the tanks contain liquids of different sound velocities then:

$$i_1(x, t) = 1 - \sin 2\pi \left( \frac{x}{\lambda} - \frac{t}{\tau} \right), \quad (7)$$

and

$$i_2(x, t) = 1 - \sin 2\pi \left( \frac{x}{\lambda'} - \frac{t}{\tau} \right), \quad (8)$$

$\lambda$  is the wavelength in  $T_1$  and  $\lambda'$  in  $T_2$ . The observed intensity

distribution in this instance is:

$$I(x) = \tau \left[ 1 - \frac{1}{2} \cos 2\pi \frac{x}{\lambda/(1-\cos \psi)} \right], \quad (9)$$

where  $\cos \psi = \lambda/\lambda'$ . The separation between intensity maxima has become larger:

$$\Lambda = \frac{\lambda}{(1-\cos \psi)} = \frac{\lambda}{(1-\lambda/\lambda')} \quad (10)$$

This suggests the possible use as a method to measure the change of sound velocity relative to a normal value.

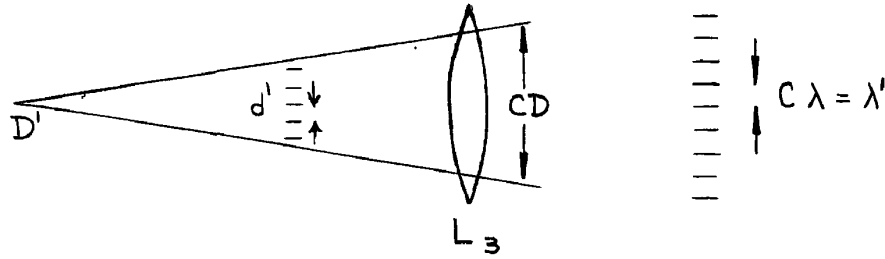


Figure 3. Tank  $T_1$  in Divergent Light.

The case where tank  $T_1$  is placed in the space between  $D'$  and  $L_3$  is treated in a similar fashion. The assumption is made that the distance the light travels through the first sound wave  $\omega_1$  is small compared with the radius of curvature of the light beam; and one neglects the fact that only the paraxial light-rays pass through the sound waves perpendicularly.

After the light has passed through the first sound wave ( $\omega_1$ ):

$$x_1 = 1 - \sin 2\pi \left( \frac{x}{\lambda} - \frac{t}{\tau} \right). \quad (11)$$

If the diameter of the cone of light rays at  $\omega_1$  is  $d$  and behind  $L_3$  is  $cd$ , then the amplification factor is  $c$ , and the wavelength  $\lambda$  at  $\omega_1$

becomes  $\lambda' = c \lambda$  after lens  $L_3$ . Therefore  $i_1$  becomes  $i_1'$ :

$$i_1' = 1 - \sin 2\pi \left( \frac{x}{\lambda'} - \frac{t}{\tau} \right). \quad (12)$$

Thus, as in the previous case for both tanks in parallel light, with a different liquid in each tank the distance between maxima becomes:

$$\Delta = \frac{\lambda}{\left(1 - \frac{1}{c}\right)} = \frac{\lambda}{\left(1 - \frac{1}{\lambda'}\right)}. \quad (13)$$

As tank  $T_1$  is moved toward  $D'$ ,  $\omega_1$  approaches the secondary source and  $d$  goes to zero, that is, the amplifying factor  $c \rightarrow \infty$  and  $\lambda' \rightarrow \infty$ ; this then gives for  $i_1'$ :

$$i_1' = 1 - \sin 2\pi \frac{t}{\tau}, \quad (14)$$

which shows that the light intensity is independent of  $x$ , and is modulated with the period  $\tau$ .

After passage through the second progressive wave  $\omega_2$  in tank  $T_2$  the intensity pattern becomes:

$$I(x) = \tau \left[ 1 - \frac{1}{2} \cos 2\pi \frac{x}{\lambda} \right] \quad (15)$$

the distance between maxima in the intensity pattern being  $\Delta = \lambda$ .

## Phase Shift upon Reflection at a Liquid-Liquid Interface

Lord Rayleigh (34) has shown that for a sound wave incident upon an interface between two liquids of velocities  $V_1$  and  $V_2$ ,  $V_1 > V_2$ , and with densities  $\rho_1$  and  $\rho_2$ , there occurs a phase shift in the reflected wave; the phase shift is zero at the critical angle and increases to  $\pi$  radians when the incident angle is increased to  $\pi/2$ .

Rayleigh gives for the incident wave:

$$\phi = \cos(ax + by + ct); \quad (16)$$

the interface lies at the  $x = 0$  plane. And for the reflected wave:

$$\phi = \cos(-ax + by + ct + 2\epsilon), \quad (17)$$

where  $2\epsilon$  is the phase difference between the reflected and the incident waves. It is given by:

$$\tan \epsilon = \frac{\rho_1}{\rho_2} \left( \tan^2 \theta_1 - \frac{V_1}{V_2} \sec^2 \theta_1 \right)^{1/2}. \quad (18)$$

The critical angle  $\theta_{1c}$  is defined by:

$$\theta_{1c} = \sin^{-1} \left( \frac{V_1}{V_2} \right). \quad (19)$$

There is also a refracted wave, or rather a disturbance, in the second liquid which penetrates little more than a few wavelengths. Arons and Yennie (35) recently measured the phase distortion of acoustic pulses reflected obliquely from the ocean bottom and found good agreement between calculated and measured pulse shapes.

## Scheme for Measuring the Phase Shift

The method for measurement of this phase shift in the present work

is an outgrowth of a technique shown by Hiedemann and Bachem (36) for comparing the effectiveness of a stroboscope. In figure 4a there is shown a wave-train incident upon a reflecting surface at an angle  $\theta_1$ , and a wave-train which is in phase with the incident waves.

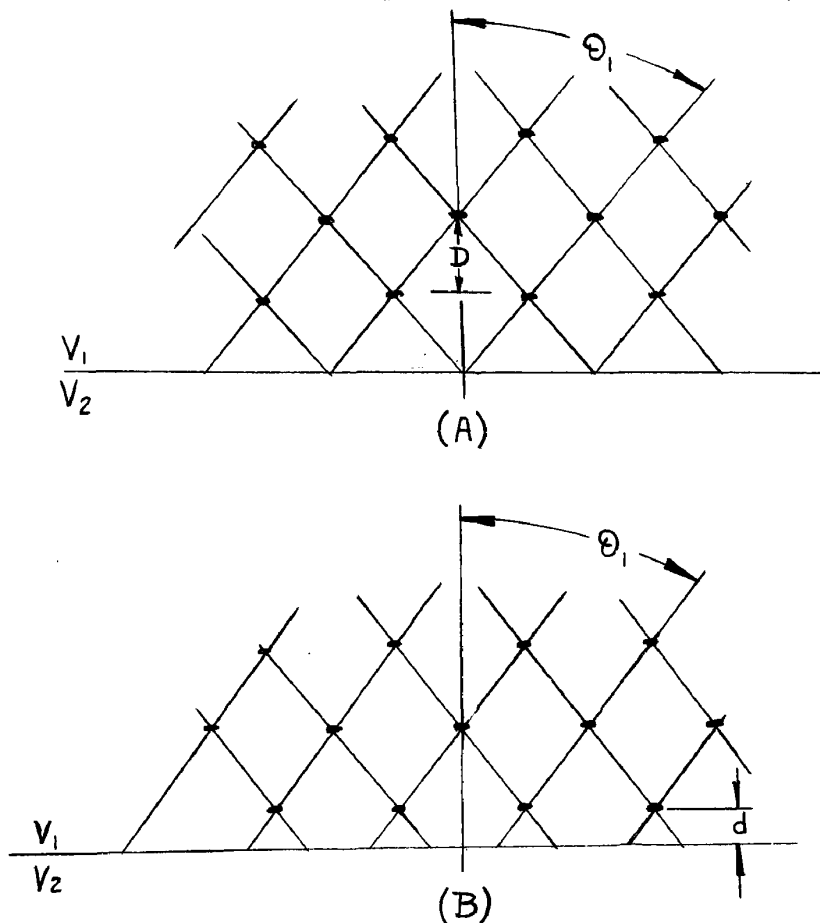


Figure 4. Interference points from incident and reflected sound beam. (a) No phase shift, (b) phase shift of  $180^\circ$ .

If this wave train is not illuminated stroboscopically the points of coincidence of the pressure nodes move parallel to the reflecting surface and one sees a set of pseudo-stationary-waves, or combination waves, which appear to be emerging from the reflector with a phase velocity equal to  $V/\cos \theta_1$ . The dots form a trace parallel to the reflector and move with a velocity  $v = V/\sin \theta_1$ . Illuminated stroboscopically the com-

bination waves disappear and there appear only the points of coincidence.

An analysis of the phase shift can be made by measurements of the spacings on a photograph according to the following sketches in figure 5.

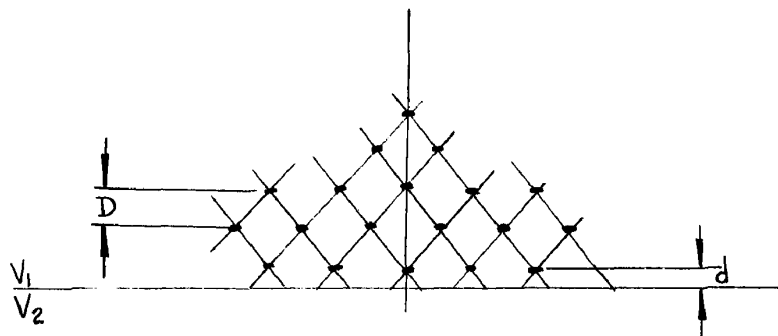


Figure 5. Measurement of D and d.

From the drawing it can be seen that one need only measure the spacings D and d perpendicular to the interface and use the relationship:

$$2\epsilon = \frac{d}{D} 2\pi = \text{phase shift.} \quad (20)$$

The phase shift is such that the dots will move away from the reflector as the phase  $2\epsilon$  increases.

## Diffraction Wavefield before a Beam Forming Quartz

The diffraction pattern in the immediate vicinity of a narrow quartz which is very long compared with the wave length is similar to that for optical diffraction by a narrow slit of infinite length. Young (37) first made the assumption that the diffraction pattern before a narrow slit could be produced geometrically by assuming an undisturbed plane wave which passes through the slit and two cylindrical waves originating at the slit edges. Sommerfeld (38) has given an exact mathematical solution for the problem of diffraction by a half-plane, and Schwarzschild (39) has calculated the case for two half-planes which formed a slit.

Osterhammel (40) considered the sound field before a beam forming quartz and found good agreement between photographs and drawings produced under the assumption that a lengthy transducer of small width ( $D$ ) will produce slit-like diffraction images. The phase relationship between the plane waves and the cylindrical waves is not clearly given by his pictures nor was it discussed.

By stroboscopic illumination of the wavefield in the immediate neighborhood of such a quartz the true character of this phase relationship should be determined. As an aid to the analysis of the photographs figures 6 and 7 were drawn under an assumed  $D/\lambda$  ratio of 11.56.

Figure 24 shows a photograph of such a beam in carbon tetrachloride; the ratio of width of quartz to wavelength is  $D/\lambda = 11.56$ . The transducer frequency was 4.42 mc/sec. Figure 6 shows the expected situation for both types of wave in phase, while figure 7 was drawn for a phase difference of  $180^\circ$  between the cylindrical and plane waves. Positions of coincidence or near coincidence of the maxima of the three waves (only



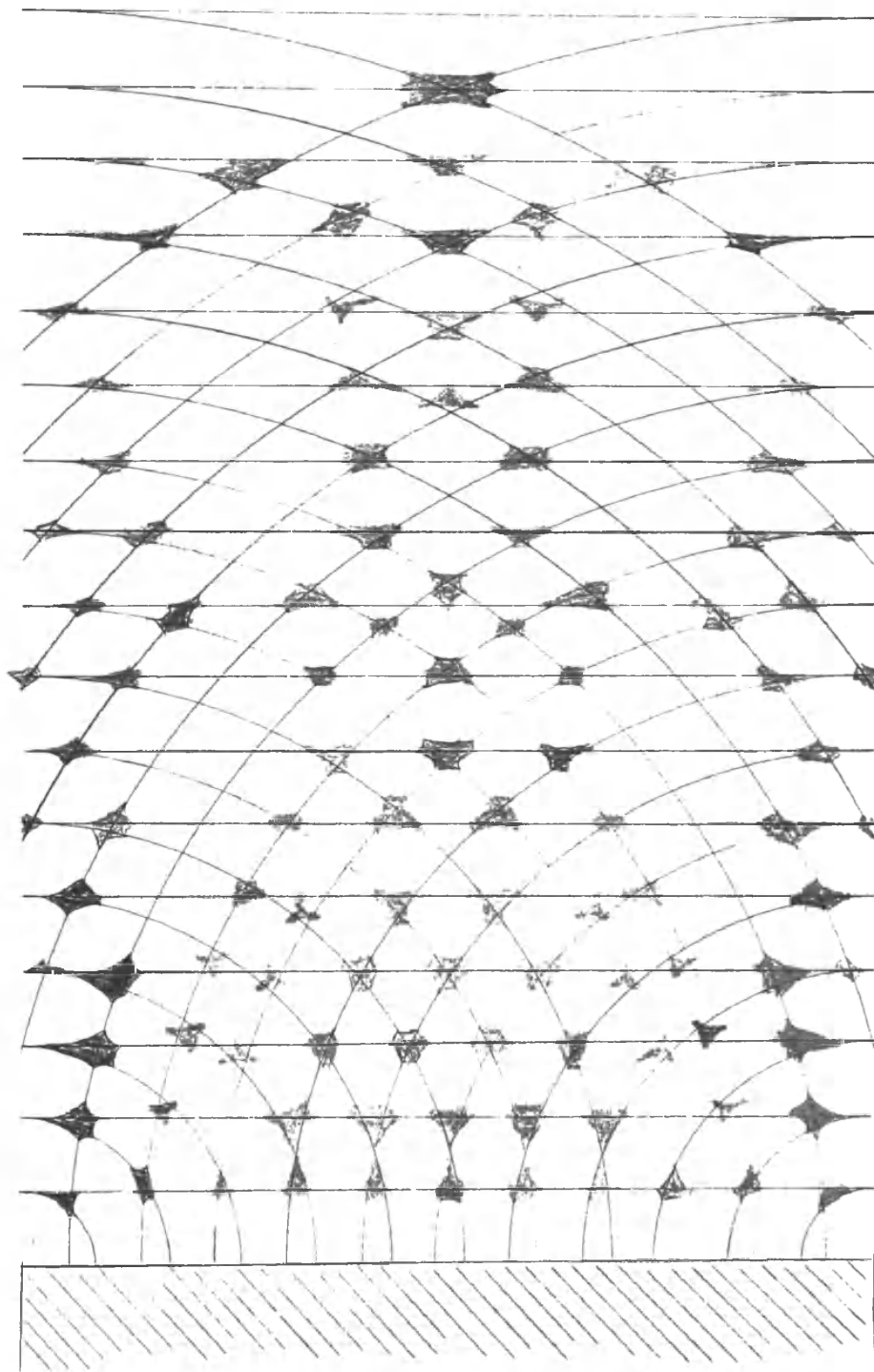


FIGURE 6. DRAWING OF INTERFERENCE POINTS FOR PLANE AND CYLINDRICAL WAVES IN PHASE

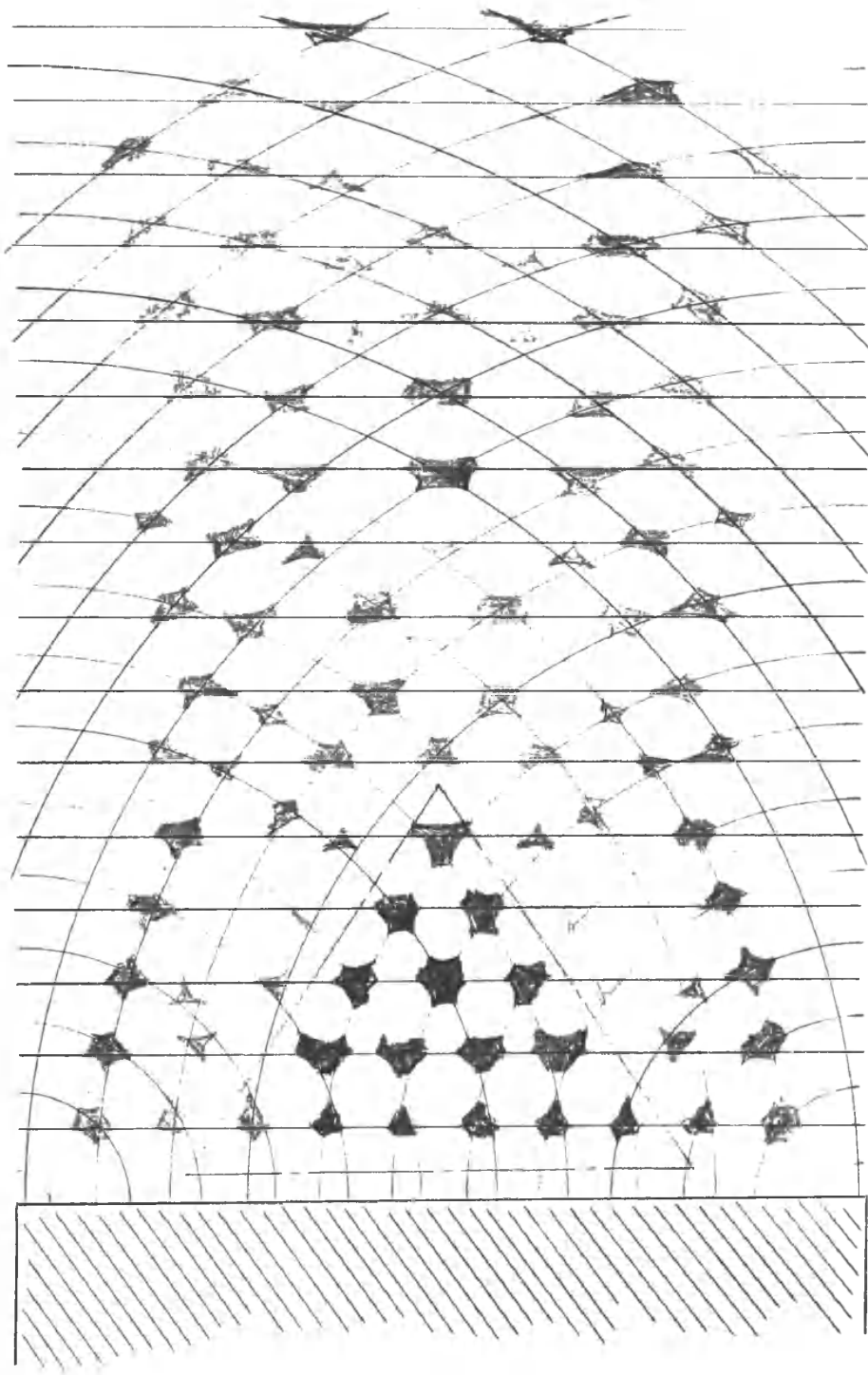


FIGURE 7. DRAWING OF INTERFERENCE POINTS FOR PLANE AND CYLINDRICAL WAVES OUT OF PHASE BY  $180^\circ$

sound pressure maxima are drawn) have been blackened. Coincidences of the maxima of two waves near a minimum of a third were shaded.

There is a clearly defined difference in the interference pattern which lies within several wavelengths of the emitting surface. In the case where there is a phase difference of  $180^\circ$ , the dot pattern at the center gives a pyramid of one, two, three and four light spots. For clarity this pyramid is enclosed in a red lined triangle. The figure for the three waves in the same phase shows the pyramid to be curved and the apex dot is missing.

Farther away from the transducer, the wave-field becomes more complex, but there are differences in the curvature of the waves in the characteristic lobes which are beginning to form. There are also differences in the angles between the sides of the lobes in the two sketches.

## Phase Change at the Focus of a Cylindrical Lens

Fraunhofer Diffraction theory for electromagnetic waves indicates that there will be a phase-shift in waves as they pass through the focus of a lens. Gouy (41) first showed theoretically and experimentally that there is a phase shift of  $\pi$  for waves passing through the focus, and  $\pi/2$  for waves at a focal line for spherical waves.

Later Reiche (42) and others further examined the problem. Reiche shows that as spherical waves approach the focus the phase of the individual waves begins to oscillate about the proper position with an increasing shift in phase difference ahead of and behind the normal position. Figure 8 gives a representation from Reiche of the theoretical

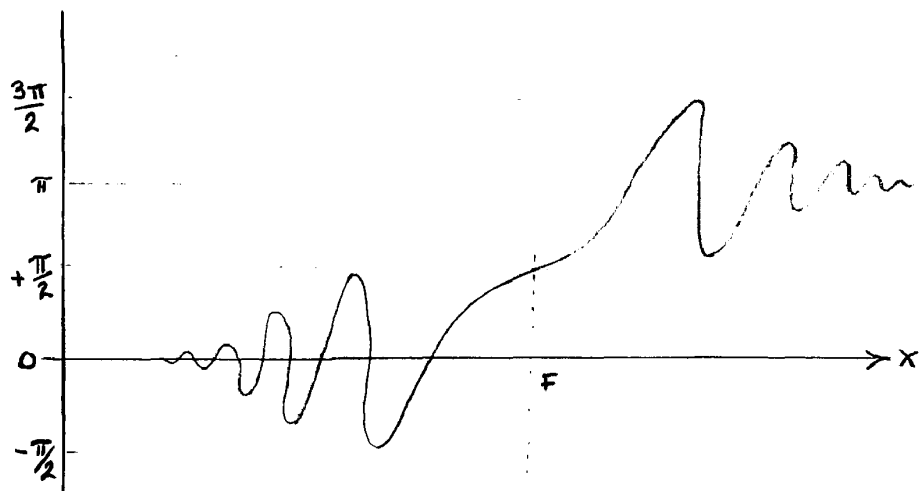


Figure 8. Phase change in the region of the focus for spherical waves (Reiche).

phase relationship near the focus. As the wave passes through the focal point the center of the phase oscillation jumps to a position  $\pi$  radians ahead of the normal positions of the wave; the phase oscillations decrease until approximately seven wave-lengths distance past the focal point where there is a normal procession of the waves outgoing from the focal point with regular phase ( $2\pi$ ) spacing between successive wave

fronts.

If one were to measure across the focal point over a distance of greater than seven wave-lengths on each side of the focal point, one should expect the distance to be  $(n \pm \frac{1}{2})\lambda$ , where  $n$  is an integer,  $\lambda$  the wave-length, and  $\lambda/2$  the phase shift which is predicted.

For the case of waves at the focus of a cylindrical lens the predicted phase change will be only  $\lambda/2$ .

## EXPERIMENTAL APPARATUS

### Oscillator and Power Supply

The oscillator was built by the author according to a composite circuit drawn from two units in the Radio Amateur's Handbook (43). See figure 9. The master oscillator is a well-stabilized, variable-frequency section in which a 6AG7 pentode is used in an electron-coupled series tuned Colpitts oscillator circuit. The inductance is tapped so that it can cover the frequency range from 1mc/sec to 3.7mc/sec.

The master oscillator is well shielded and is mounted on a chassis together with three doubler stages using 6V6's, and a power-amplifier stage of two type 807 tubes in parallel. A switch permits the selection of one, two, or three doubler stages so that the total frequency range at the output is 1-28mc/sec. The first doubler is always in use and at low frequencies may serve as a buffer-stage between the master oscillator and the power output stage. The second and third 6V6's are triode-connected. The 6Y6 tube is a protective device which raises the grid bias on the 807's when no signal is present at their grids. The radio frequency power at the power amplifier is nominally one hundred watts.

The power supply consists of two units mounted on separate chassis. Figure 10 gives the circuits for both units. One unit furnished 400 volts with a small degree of regulation; the other unit provides a continuously variable voltage of from 0-700 volts. It is estimated that powers up to 150 watts can be furnished by this latter unit.

A similar power amplifier, built by A. P. Loeber, was used to excite the stroboscope quartz. It was driven by the same master oscillator.

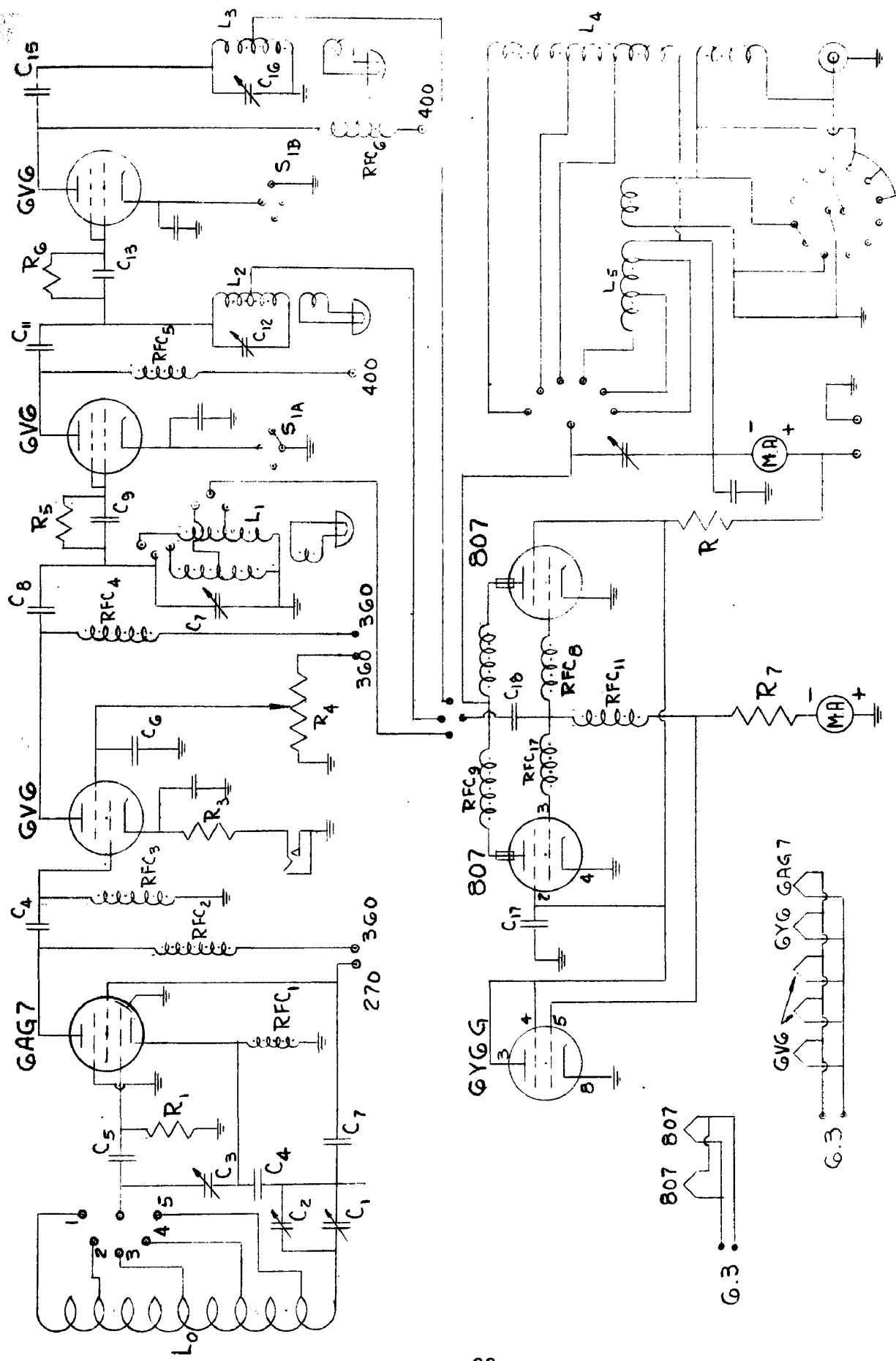


FIGURE 9. CIRCUITS OF OSCILLATOR AND AMPLIFIERS





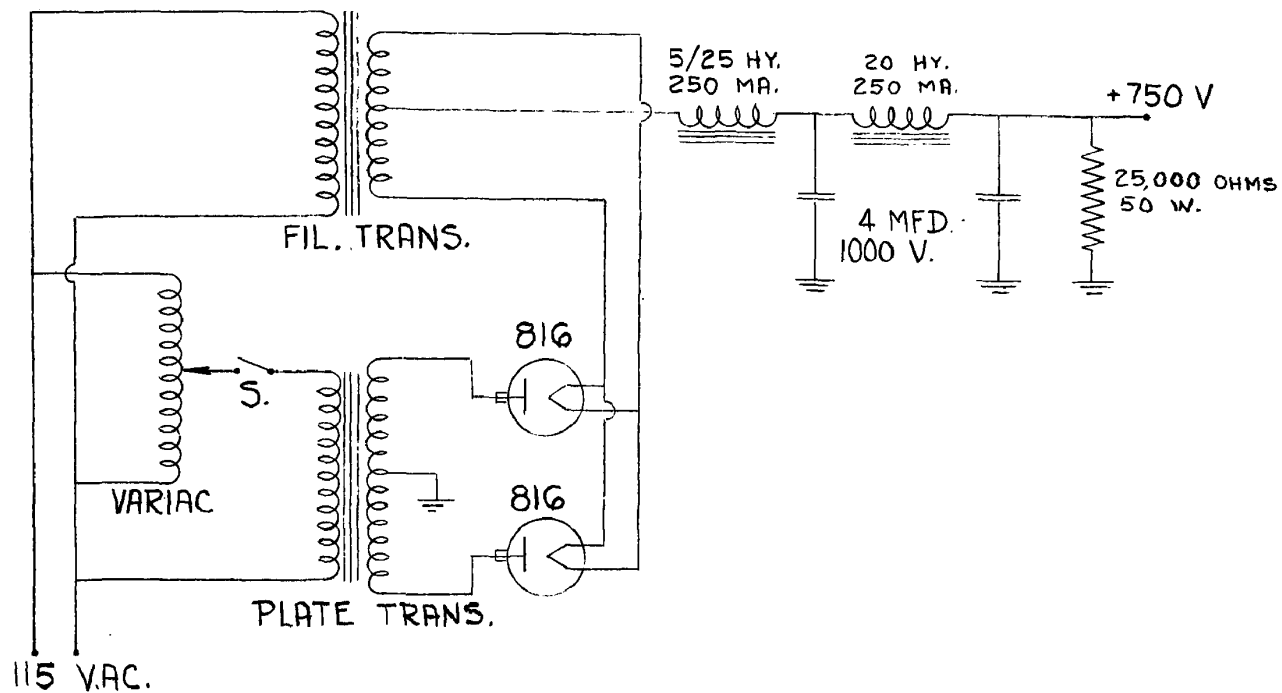


FIGURE 10 b. HIGH VOLTAGE POWER SUPPLY

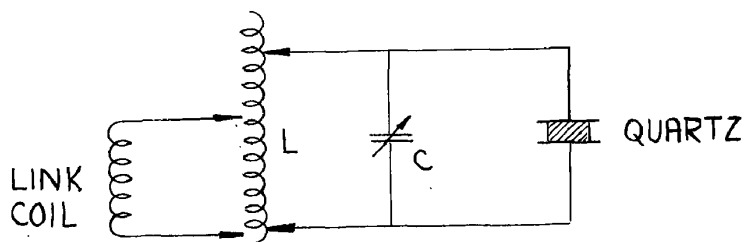


FIGURE 11. IMPEDANCE MATCHING CIRCUIT

The use of separate drivers for the two tanks made it possible to operate  $T_1$  and  $T_2$  independently, and to provide different sound intensities from the two quartz transducers.

### Optical Equipment

The lenses are described elsewhere, and need no special comment here.

The optical bench with associated riders, bilateral slits, and micrometer-screw traversing riders were manufactured by Spindler and Höyer, Germany. The light source used was a high pressure mercury lamp A-H4; for certain portions of the experimental work, a Gaertner filter set L541 E was used to transmit the Green line of mercury 5461  $\text{\AA}$ .

Almost all of the photographs were taken with an Exacta model VX with lens removed. Other lenses of more suitable focal length were held in holders and mounted on riders. This camera had the advantages of a copious film supply to permit many exposures and a focal-plane shutter with speeds up to twelve seconds.

### Ultrasonic Equipment

The transducers were in all cases x-cut quartzes of one half, three quarter, and one inch square. The beam patterns were produced by a special 71° x-cut quartz of one inch length. This quartz is used because the vibrating surface lies perpendicular to the direction of minimum Young's modulus, therefore the maximum amplitude is obtained. But most important, this cut of quartz has a more piston-like vibration than any other cut. This is the same type crystal used by Osterhammel (40) in his work.

## DISCUSSION

### Comparison of Two Velocities

In his discussion of the situation where both of the tanks are placed in collimated light and the progressive sound beams are parallel with each other and perpendicular to the light rays, Bär (1) suggested its use as a method for measuring, or for comparing two velocities of sound. The two velocities might be for two different liquids, or of the same liquid at different temperatures in each of the tanks. Another possibility is that for measuring diffusion rates of one liquid into another, in which case the sound in  $T_2$  would be transmitted parallel to the diffusion layer. The velocity change across the boundary being a function of the diffusion at the boundary.

Although the present method has not been cited as having been used before, Giacomini (33) has reported measurements made on a single liquid in which he employed two quartzes radiating progressive waves side by side in opposing directions. In this case the value of  $\mathcal{L}$  remains constant at  $\lambda/2$ .

Equation (10) from above was:

$$\mathcal{L} = \frac{\lambda}{(1 - \lambda/\lambda')} \quad (10)$$

Substitution of  $\lambda = v/\nu$  and  $\lambda' = v'/\nu$  into equation (10) gives  $\mathcal{L}$  in terms of frequency  $\nu$  and the velocities  $v$  and  $v'$  in tanks  $T_1$  and  $T_2$ :

$$\mathcal{L} = \frac{1}{\nu} \frac{vv'}{v' - v} \quad (21)$$

This relationship is shown in the plot on Figure 12, where  $v'$  is taken equal to 1500 m/sec as a parameter; the graph is for  $\Delta$  versus  $\Delta v = v' - v$ . It shows clearly the sensitivity of this method for small velocity differences, and indicates the necessity for a longer wave-field. More exact measurements should be possible if the optics from a polariscope of the type for stress analysis in plastic models were used. A field of 17 centimeters could easily be obtained. Such a field would permit a distribution of the error, produced when selecting the center of an interference fringe, over many more fringes. The calculations given in Table 1 make use of from three to twelve fringes in a field of 12.6 cm length.

Figure 13 shows a series of photographs for a few common liquids at frequencies in the range 1-15 mc/sec. Unequal temperatures in the sound fields of one, or of both, tanks caused the curvature in the fringes of Figure 13(d). The defect can be avoided to a great degree by the use of stirring action in the liquids and with transducers which radiate a more homogeneous beam. The common technique for improving the homogeneity of a sound beam, that of placing a thin sheet of glass or metal into the sound path at an angle did not work well here, because in addition to the reflection out of the main beam of spurious rays, the thin sheet also caused attenuation of the sound and reduced thereby the contrast of the fringes. It should be noted that if the plate is flawless and homogeneous the attenuation can be neglected.

Measurement from the photographs in Figure 13 are grouped together in Table 1.

Assuming a greatest possible temperature error of 1% in each of the velocities and an error in the frequency measurement of a tenth of one

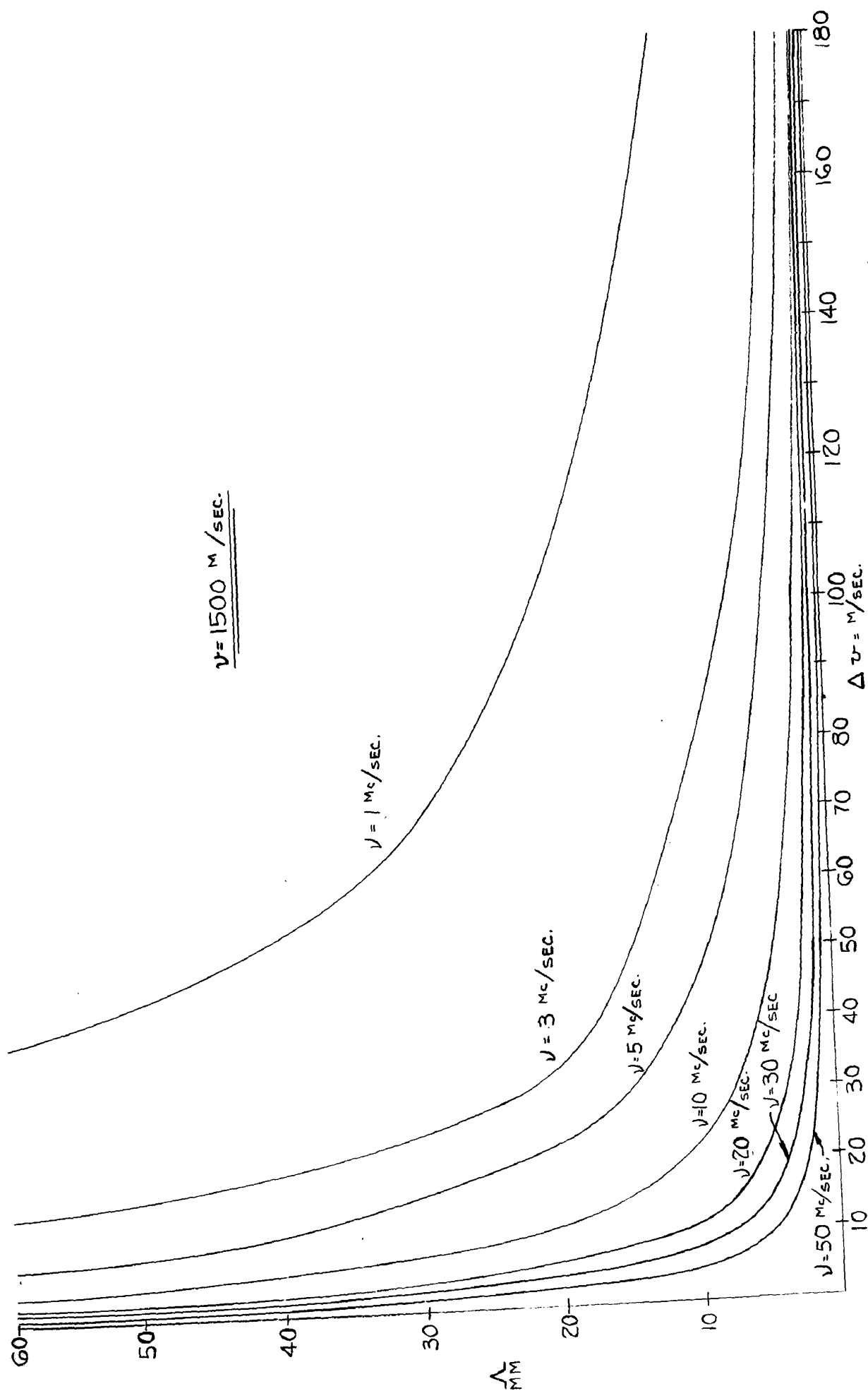
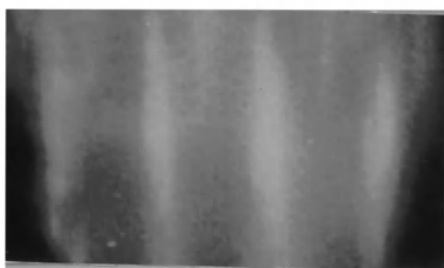
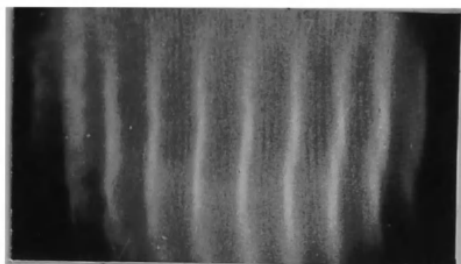


FIGURE 12. THEORETICAL CURVES FOR VELOCITY COMPARISON



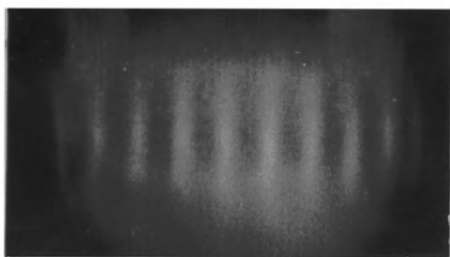
(a)

Xylene-Acetone  
 $\Delta v = 160$  m/sec  
 $v = 1.025$  mc/sec  
 $\Lambda_{\text{meas.}} = 9.51$  mm



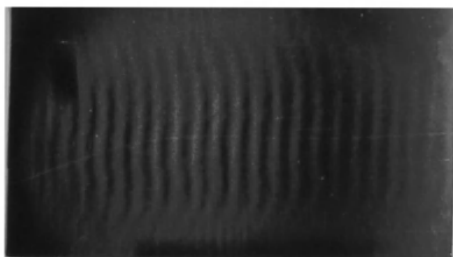
(b)

Xylene- $\text{CCl}_4$   
 $\Delta v = 394$  m/sec  
 $v = 1.025$  mc/sec  
 $\Lambda_{\text{meas.}} = 3.76$  mm



(c)

m-xylene-  
 n-propyl alcohol  
 $\Delta v = 116$  m/sec  
 $v = 3.48$  mc/sec  
 $\Lambda_{\text{meas.}} = 3.98$  mm



(d)

m-xylene-  
 n-propyl alcohol  
 $\Delta v = 117$  m/sec  
 $v = 8.87$  mc/sec  
 $\Lambda_{\text{meas.}} = 1.646$  mm

Figure 13. Photographs of Fringes for Calculating Velocity Differences.

Table 1.

	$v'$ m/sec	$v$ m/sec	$\Delta V$ m/sec	T °C.	$v$ mc/s	$\lambda$ calc. mm	$\lambda$ meas. mm	Difference %
a. Acetone	1148			28				
Xylene (mixture)		1308	160	28	1.025	9.16	9.51	3.7
b. CCl <sub>4</sub>	914			28				
Xylene (mixture)		1308	394	28	1.025	2.96	3.76	21.5
c. n-propyl alcohol	1189			28.5				
m-xylene		1305	116	28.5	3.48	3.85	3.98	3.3
d. n-propyl alcohol	1187			29.1				
m-xylene		1304	117	28.9	8.87	1.49	1.65	9.2

percent, the computed value of  $\lambda$  should be in error by less than 4%. The measured values of  $\lambda$  will be expected to lie between 5% for broad lines where only four fringes can be used and 1.0% when fringes are narrow and there are twenty fringes available. The measurements for in Table 1 were made rather coarsely on photographic enlargements by means of vernier calipers which could be read with an accuracy of a tenth of a millimeter. The frequencies given were taken from a General Radio Wave-meter, Model 566-A. A brass rod 12.71 mm diameter was placed in the field and photographed as a reference length for the calculation of  $\lambda$ .

The photographs and theoretical curves are sufficient to predict that, for a 20 mc/sec frequency, with two liquids having a  $\Delta v$  of 20 m/sec and therefore a  $\lambda \approx 5$  mm, there will be 25 fringes in a field of 126 mm width. A large error of 10% in the selection of the center, or edges, of the first and last fringes would give only 0.4% error in  $\Delta v$ , or 6 m/sec for  $v = 1500$  m/sec.

The method would give greater accuracy for higher frequencies and for a longer wave-field, but each of these factors is limited. The upper frequency is determined by an available quartz transducer which can radiate the large sound intensities needed to produce fringes of sufficient contrast to be photographed. Quartz crystals of low fundamental frequency are durable when strongly excited but have increasingly small efficiencies at their harmonic frequencies; an x-cut quartz with fundamental at 30 mc/sec is extremely fragile. Further, with low power radiation and poor contrast in the fringes a longer exposure is necessary, consequently the temperature of the liquids would change. Since the coefficients for velocity change due to heating are likely to be different for the two liquids, there will result a variation of  $\Delta v$ . A serious



application of this method would require an elaborate apparatus for temperature control.

The liquids which are to be compared might limit one or both of the factors if either of them presented relaxation effects at the higher frequencies; such liquids as castor oil (44) would be troublesome by virtue of high absorption for sound at even moderate frequencies and relatively narrow optical fields.

## Tank<sub>1</sub> in Divergent Light

That portion of Bär's paper in which the first tank  $T_1$  is placed between  $D'$  and  $L_3$  in Figure 2 has its principal value in the present work by being another test for the velocity comparison method. The interference fringes seen in the field of tank  $T_2$  are the result of an optical enlargement of the wavelength  $\lambda_1$  to  $\lambda'_1$  with consequent change in fringe separation  $\Lambda$ . It is apparent from Figure 14 that  $\lambda_1$  approaches  $\lambda'_1$  when  $T_1$  is closest to  $L_3$  and therefore  $\Lambda$  becomes infinitely large.

The method for taking measurements can be explained by considering Figure 14 below. The distance  $d$  was measured by means of a simple meter-stick from the center of  $L_3$  toward  $D'$ ; a meter-stick was sufficient for this because the lens  $L_3$  which was used had a focal length equal to 30 inches. This lens afforded a large range for the values of  $d$ , the distance of  $T_1$  from  $L_3$ .

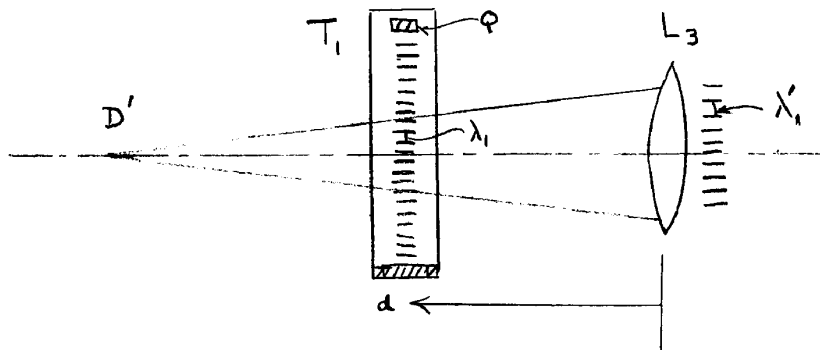


Figure 14. Relationship between  $\lambda_1$  and  $\lambda'_1$ .

Equation (13) again is:

$$\Lambda = \frac{\lambda}{(1 - v/c)} = \frac{\lambda}{(1 - \lambda/\lambda')} \quad (13)$$

where  $\Lambda$  is the distance between fringes, and  $c$  is an amplification factor. Since  $L_3$  collimates the light from  $D'$ , the distance from  $L_3$  to  $D'$  is equal to the focal length of  $L_3$ , and we can set:

$$\begin{aligned} d_{\max} &= f_{L_3} \quad \begin{cases} \Lambda = \lambda \\ c = \infty \end{cases} \\ d = 0 &\quad \begin{cases} \Lambda = \infty \\ c = 1 \end{cases} \end{aligned} \quad (22)$$

these are conditions for  $\Lambda$  and  $\lambda$  which fulfill equation (13).

A relationship between  $d$  and  $c$  which will satisfy (22) is:

$$c = \frac{1}{1 - \frac{d}{d_{\max}}} = \frac{1}{1 - \frac{d}{L_3}}. \quad (23)$$

Substitution of equation (23) into (13) gives the following:

$$\Lambda = \frac{\lambda}{1 - \left(1 - \frac{d}{L_3}\right)} = \frac{L_3 \lambda}{d}, \quad (24)$$

which is the equation of an hyperbola if  $L_3$  and  $\lambda$  are constants.

Carbon tetrachloride was used in both tanks and the quartz transducers were excited at 3.0 mc/sec. Measurements of  $\Lambda$  were taken directly from  $2\frac{1}{4} \times 3\frac{1}{4}$  film by means of a comparator whose accuracy was better than .001 mm. The measurement of  $\Lambda$  for  $d = 5.5$  cm had a possible error of 20% because only three fringes were present on the film, but this point does fit well on the curve. That for  $d = 10$  cm had eight fringes and a highest probable error of 2%. The errors for the larger values of  $d$  are approximately 1 - 5% depending upon the number and sharpness of the fringes. No stirring was used in  $T_1$  so that heating effects distorted portions of the field. The heating limited in some cases the number of fringes which could be used and lowered the expected accuracy. The data is plotted in Figure 15. Because this section of Bär's work

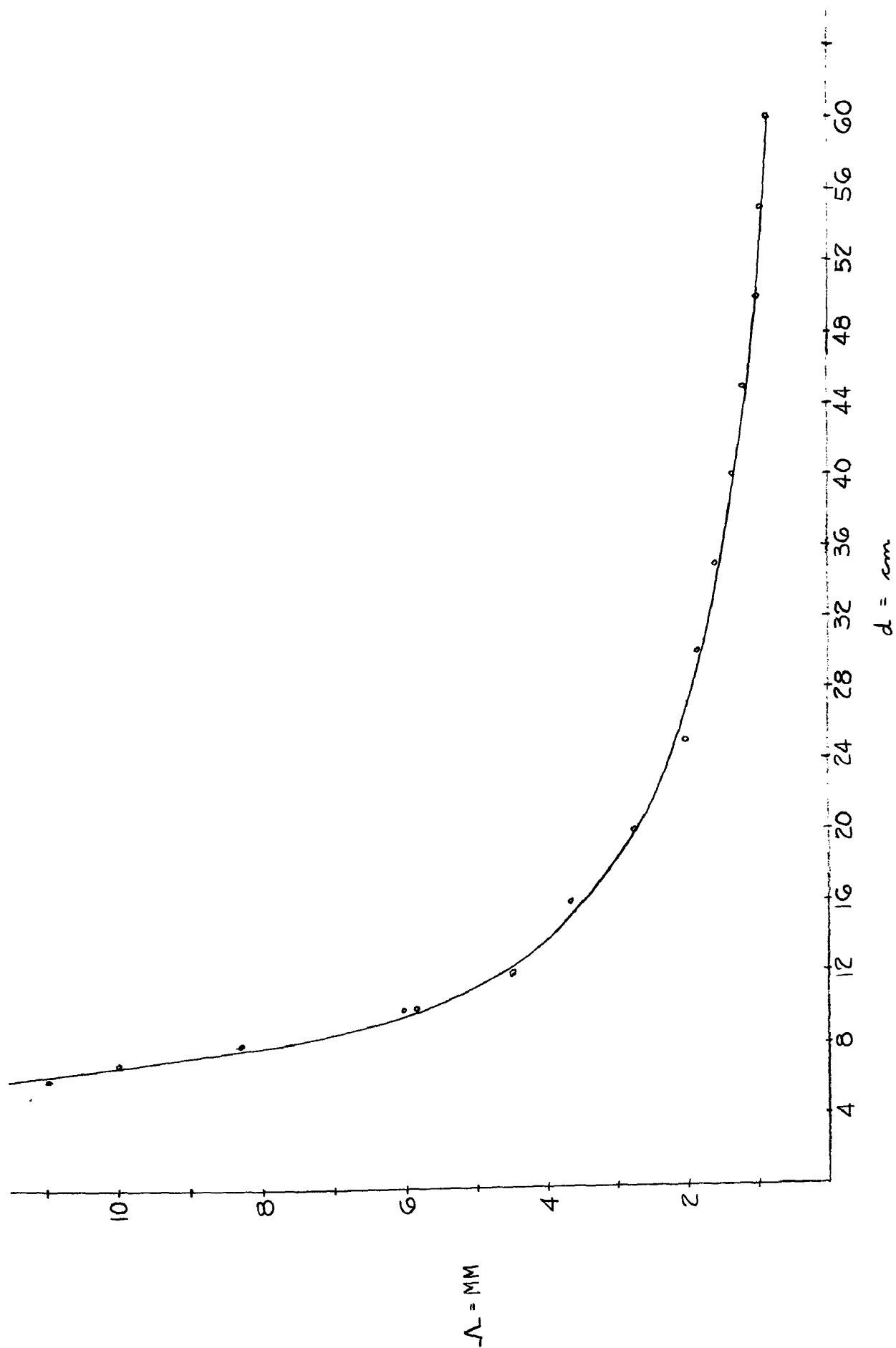


FIGURE 15. EXPERIMENTAL CURVE FOR  $\alpha$  VERSUS  $\lambda$

was of minor importance to the purpose of this thesis, it was not deemed necessary to seek greater accuracy. The data as plotted fit an hyperbola well.

Although there appears to be no immediate use for the results of this work, it should be noted the Fox and Roch (32) have employed a lensless system wherein light from a thin incandescent filament is passed twice through a sound beam before it falls upon a photographic film. Simple measurements of line spacing on the film and of the distances in the optical system provide a measure of the sound wavelength for a calculation of the velocity of sound.

Bär Stroboscope:  $T_1$  at D'

Credit is given to Bär (1) for this method of producing a stroboscopic light source; for, although Tawil (30) in 1930 was able to photograph a sound wave in air by passing light from a small source twice through the sound beam, it was Bär who gave the thorough discussion of the theory and used the first tank  $T_1$  at D' in order to obtain an overall stroboscopically illuminated field. It must be noted also that during the same year, 1936, but previous to Bär, Maercks (45) and Cermak and Schoeneck (31) used an arrangement whereby a light beam traversed two soundbeams.

Lucas and Biquard (46) discovered a broadening of a narrow light beam as it passed through a sound field and explained it as being due to refraction. Recent work by Kolb and Loeber (47) and by Loeber and Hiedemann (48) has extended the explanation of the broadening of the narrow light beam. The latter authors have used the theoretical approach due to Wiener (49).

Their explanation of the Lucas-Biquard effect is that the narrow-beam is deflected by a continuously varying index of refraction which is present in a half wavelength of sound. As the progressive sound wave moves past the narrow beam of light, both the gradient of index of refraction and its sign change periodically. Thus the narrow light beam is deflected horizontally to each side of a normal zero position once during a period.

Bär suggests the frequency limits of 1 mc/sec and 20 mc/sec when tank  $T_1$  is at D'. The lower limit because the bending of light in the sound-field at this frequency would be small; the upper limit because sufficiently high sound intensities are difficult to attain above this

frequency. Contradictory to this lower limit is the fact that Loesber (50) obtained large deflections of a narrow beam at 400 kc/sec.

Using a second optical arrangement given by Bär which is similar to Figure 16, a camera was placed at D such that an image of the space

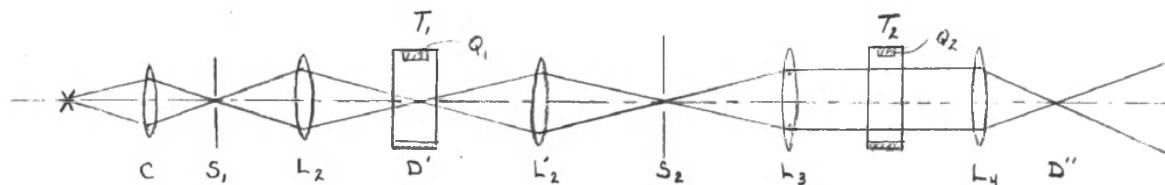


Figure 16. Revised Optical Arrangement by Bär.

at  $S_2$  was in focus. The photographs in Figure 17 show the slit image at  $S_2$  for various sound intensities present in  $T_1$ . The greater deviation of the slit image with increase in sound intensity in  $T_1$  is expressed here as a broadening of the slit image.

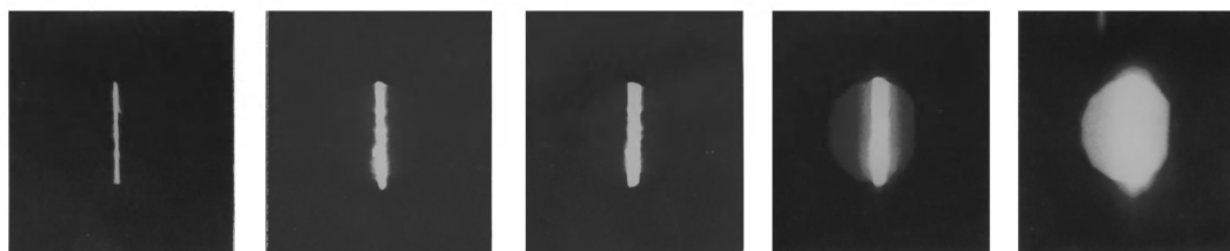


Figure 17. Broadening of Slit Image.

A method for comparing the effectiveness of a stroboscope has been given by Hiedemann and Bachem (36). The duration of light during each cycle is given by comparing the length of a dot-trace with the distance between dot-centers. The ratio of dot length to separation of centers will give the fraction of the sound period during which the light is transmitted through the combination waves. Pictures of these waves are shown in Figure 18; they were taken at two different frequencies, using the optical arrangements suggested by Bär.

It is difficult, as it is evident from Figure 18 (b), to obtain a field of light which is illuminated with an even intensity and with light of equal duration. Examples of this can be found also in Figures (19) and (20) showing sound waves through a lens and a diffraction grating.

To use the optical arrangement in Figure (16) one first needs to adjust the sound beam until it is perpendicular to the axial rays of the cone of light at D' and until the wave-fronts are parallel to the slit S<sub>1</sub>. If the latter adjustment were to be neglected, the different portions of the slit image at D' would not all be in the same phase.

Slit S<sub>2</sub> is then traversed until the best stroboscopically illuminated field is obtained. These adjustments can be made either with standing waves present in T<sub>2</sub> or with the sound waves in T<sub>2</sub> being reflected from the bottom of the tank, in which case pseudo-stationary waves will be formed, and the dot-pattern will appear as a measure of the stroboscopic action of T<sub>1</sub>. When stationary waves are used in T<sub>2</sub> the fringe spacing will be  $\lambda/2$  for non-stroboscopic light and  $\lambda$  when the quartz in T<sub>1</sub> is well adjusted. As the adjustment is improved, half of the fringes will disappear.

Bär states that the cross section of the light beam at the focus (D') must be less than  $\lambda$ . According to the findings of Loeber and Kolb (47) the cross section of the light beam should be less than  $\lambda/2$  for best results.

Because the width of the transducer is a factor in determining the cross section of the light beam within the sound beam, tests were made using one inch, three quarter inch, and one half inch square quartzes and best results were attained using the one half inch square quartz. A one half inch quartz with one quarter inch electrodes produced less ill-



umination, but no significant improvement in the stroboscopic action could be noted. A longer quartz (perhaps one inch) of only one half inch width should improve the light intensity without harm to the action of the cell. Again, a one inch square quartz with only a one-half inch electrode was applied with unsatisfactory results. The failure of narrower electrodes may be attributed to unusual wave forms having been emitted, or to a sound beam which was wider than the electrode.

Naturally, the focal lengths of the lenses used and their positions on the optical bench must be selected with care. Generally one seeks the lens components which by their positions and aperture will give the greatest amount of light and the narrowest beam-cone at D'. For this reason  $L_2$  should be in its near position to  $S$ , and lenses  $L_2$  and  $L_3$  should be of longest focal length consistent with a large aperture. An American Optical Company objective of 10 inch focal length and 2 inch diameter and an achromat of 19 inch focal length and two and five sixteenths inch diameter were used most often for  $L_3$ . A six and one half inch American Optical Company objective was used for  $L_2$ . The condensor lens system C is that from a Spencer Projector when using 35 mm slides.  $L_2$  was an eight and one half inch achromat, or a three and one half inch,  $f/3.5$ , objective set from a surplus gunsight.

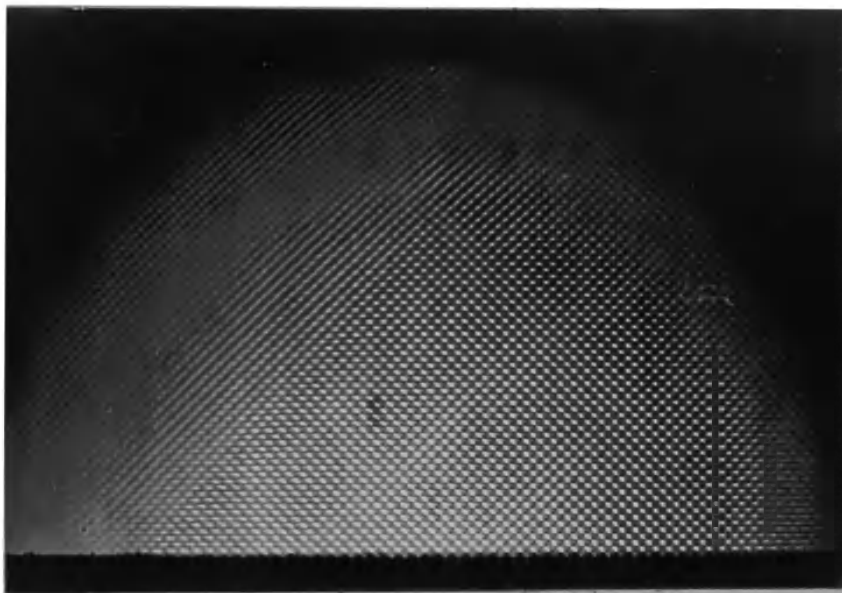
Best action resulted when the light beam passed the face of the quartz at a distance of approximately two to four millimeters. When this proximity is used, stirring action is necessary in the stroboscopic cell  $T_1$ , since heat-schlieren will tend to reduce the shutter action of the sound waves.

Stationary sound waves in  $T_1$  were used in a short series of test. It is possible to use this arrangement to effect stroboscopic lighting,

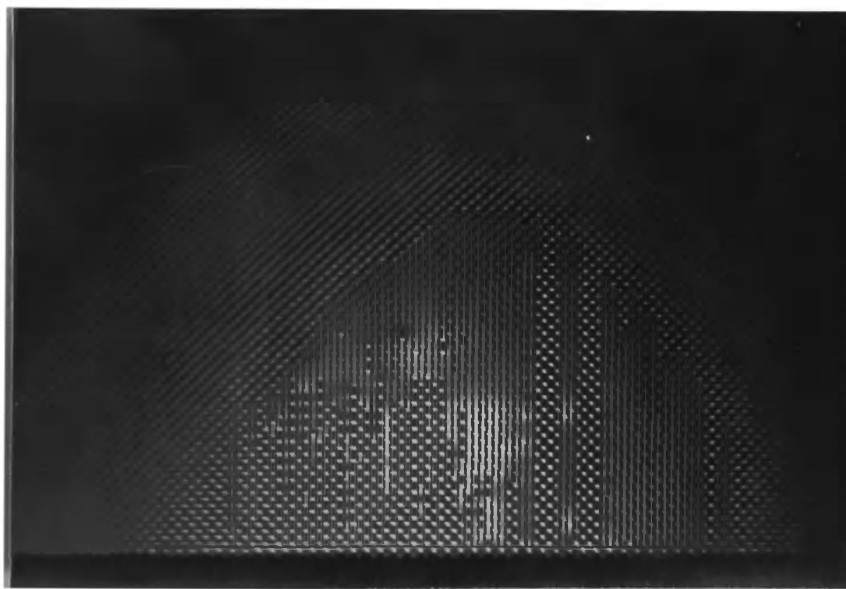
but an additional adjustment is required. The stationary waves must stand in tank  $T_1$  such that a sound pressure node is at  $D'$ . Here too also would be found some of the difficulties mentioned by Goudet (18). The spacing between reflector and transducer must be adjusted, and heating in the liquid tends to change this adjustment. The use of progressive waves is much more simple.

Examination of Figure 18 (a) leads one to expect stroboscopic illumination with a period of  $2.26 \times 10^{-7}$  seconds and a duration of  $4.77 \times 10^{-8}$  second. In Figure 18 (b) it is possible to estimate  $\tau = 5.5 \times 10^{-8}$  second. Perhaps the one great advantage of this stroboscope is the increase in illumination. The best pictures shown by Hiedemann and Bachen (36) were taken with exposure times of ten to twenty seconds. In the present work exposure times of one-twenty - fifth of a second to four seconds were always sufficient.

Figures 19 - 21 are given merely as examples of the effectiveness of the stroboscope.



a. 4.42 mc/sec



b. 2 mc/sec

Figure 18. Photographs of Interference Points

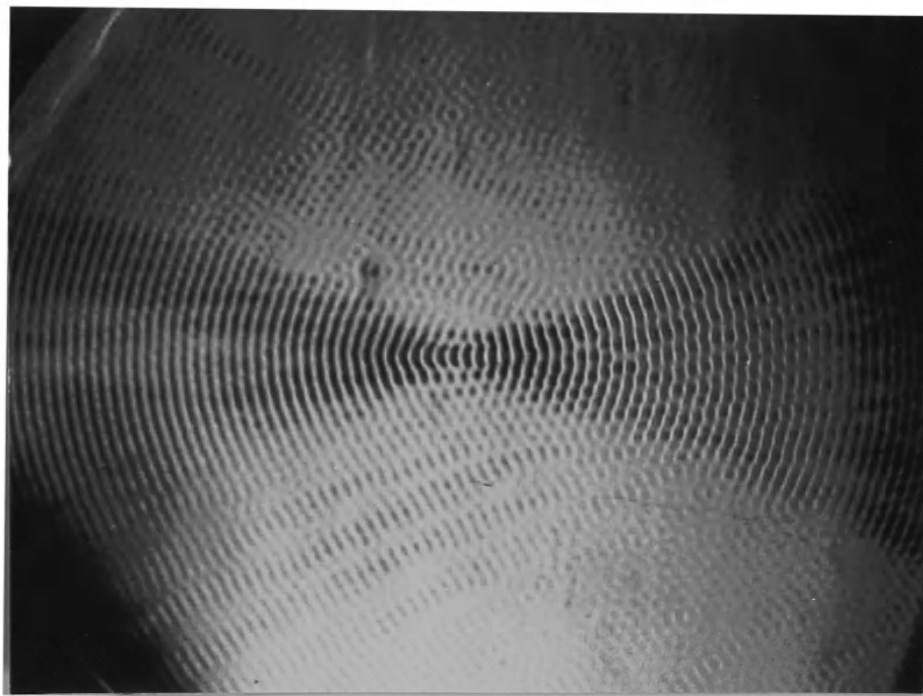


Figure 19. Sound Waves Focused by Cylindrical Plastic Lens.

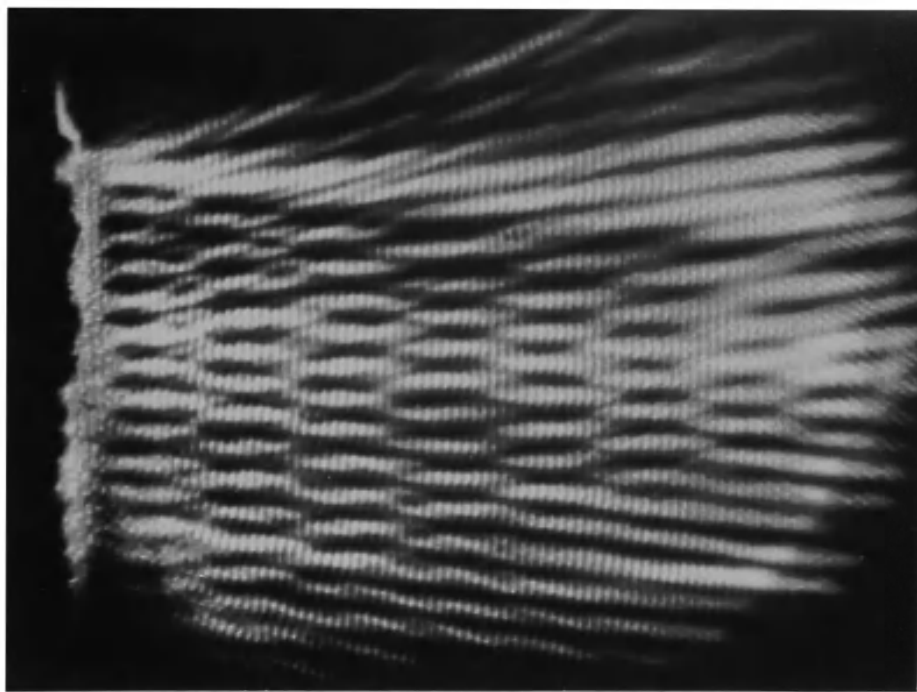


Figure 20. Sound Diffraction Grating.

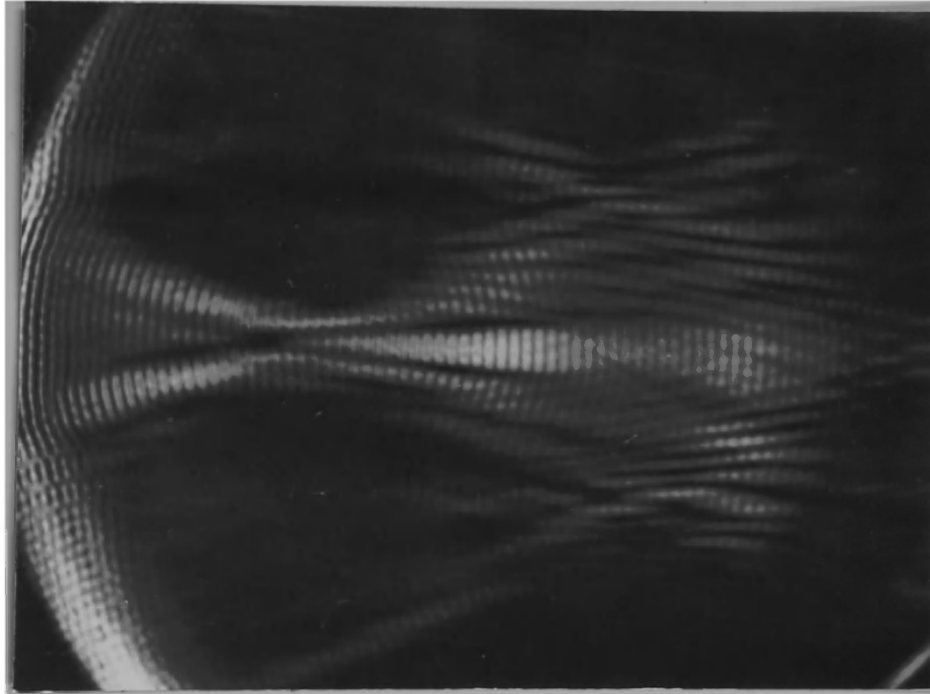


Figure 21. Diffraction Orders Brought to Focus by a Lens.

### Raleigh Phase Shift

An interface between glycerin and carbon tetrachloride was chosen because of the extreme difference between their velocities, 1914 m/sec and 923 m/sec, respectively, at 25° C. This large difference gives a low critical angle:

$$\theta_{ic} = \sin^{-1} \frac{V_1}{V_2} \approx 28^{\circ} 30' \quad (19)$$

The advantage of a small critical angle is obvious upon inspection of the dotted theoretical curve for  $2\epsilon$  in Figure 22. The smaller critical angle permits a larger range of incident angles from  $\theta_{ic}$  to 180°. Incident angles greater than 75° produce dots which are large and elongated; this reduces the accuracy of measurement to such an extent that no data was taken above 73°.

Although the glycerin will float very nicely above the  $\text{CCl}_4$  in the tank, it was impossible to work this simply because surface tension between the glycerin and  $\text{CCl}_4$  caused a meniscus at the tank wall to pull downward to such a depth that it was impossible to get an image of the interface between the two liquids.

A square brass tank, 2 x 3 inches by 1 inch high, was made and a mica window was cemented to the bottom. The mica was a section which was peeled from a thick sheet until it was of uniform thickness. A thickness of 0.06 mm was thought to be sufficiently thin to behave like a thin film. Assuming that the velocity of sound in mica to be 4000 m/sec the wavelength at 3.0 mc/sec would be  $\lambda = 1.33 \text{ mm}$ .

The use of this tank with mica window made it possible to obtain a sharp image of both the reflecting layer and the dots formed by the waves. A sharp image of this boundary was most important for measurement of  $d$ ,

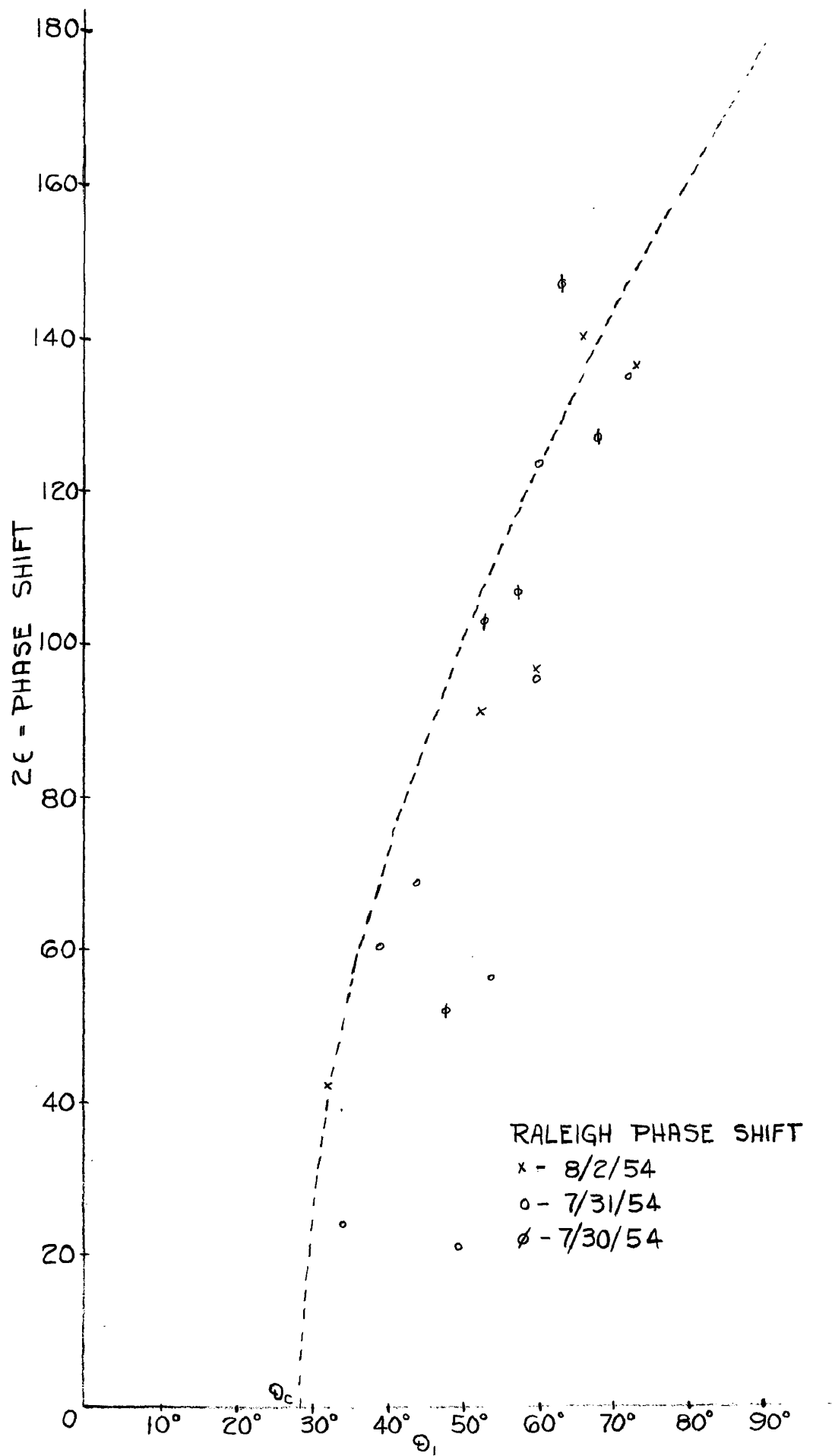


FIGURE 22. EXPERIMENTAL CURVE FOR  $\Theta_1$  VERSUS  $2\epsilon$



the distance from reflector to the first row of dots.

The measurements for  $D$  and  $d$  were made by a means of a comparator from 35 mm photographic film, and the angles of incidence were made on photographs. Three measurements were taken and the simple averages of  $D$  and  $d$  were used to compute  $2\epsilon$ . The principal error arose from the estimation of the center of the dots. The greatest probable error for the measurement of  $2\epsilon$  was 10%.

It will be seen that the data on Figure 22 follows the theoretical dotted curve well except for a few points in the region of  $50^\circ$  and  $60^\circ$  where the agreement is extremely poor. This can be explained if we assume, in spite of the apparent effectiveness of the mica to work as a thin film between the two liquids, that there occurs at the troublesome angles a form of vibration in the mica itself.

It has been shown by Cremer (51) and Götz (52) that a necessary condition for sound transmission through thin sheets is that the trace velocity of the incident and reflected waves at the boundary of the sheet be equal to the velocity of a vibrational mode within the sheet, or in the surface. A common mode of vibration is flexural vibration in which the sheet acts as a wave guide for the sound; the sound waves ricochet through the sheet with a velocity  $V$  producing a flexural motion with velocity  $v = V/\cos \theta_2$  parallel with the boundary;  $\theta_2$  is the complement of the angle of refraction in the sheet, and  $V$  is the ordinary longitudinal or shear wave velocity in the sheet. This mode is excited when  $v$  is equal to the trace velocity.

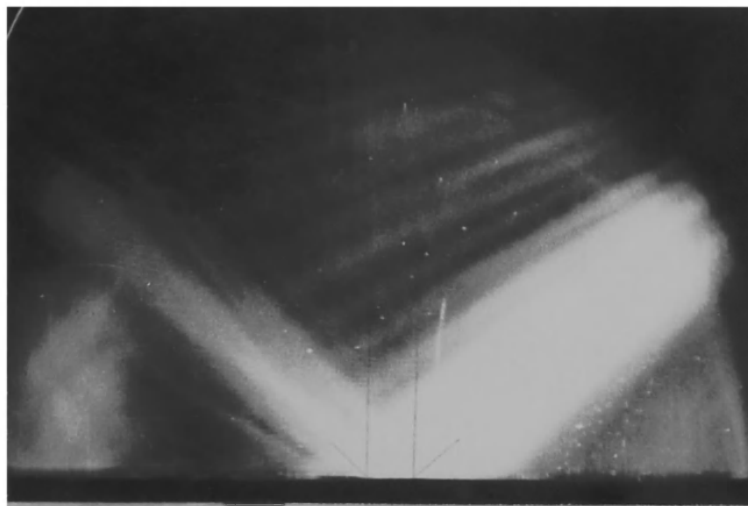
Another common mode is that of Rayleigh surface waves. These are transverse waves in the boundary and extend only a few wavelengths into the boundary.

Flexural waves produce a non-specular reflection of the incident waves, while Rayleigh waves displace the reflected waves, so that the incident and reflected sound beams do not have the same normal at the surface.

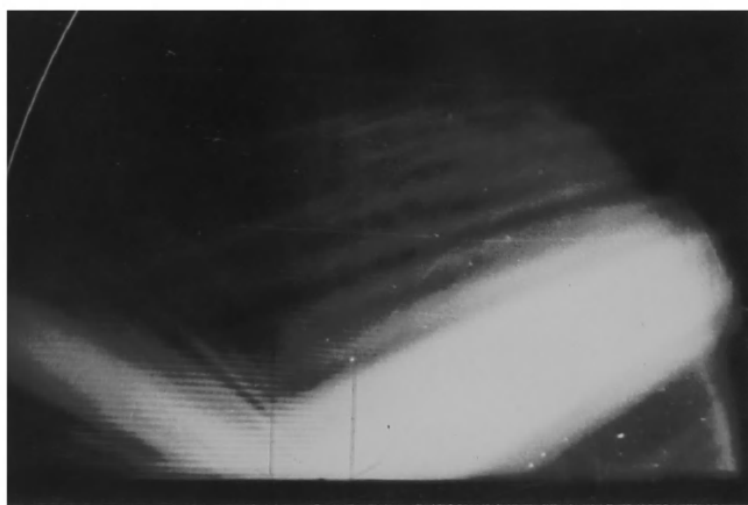
Naturally, when the one of these waves is excited the phase of the reflected wave with respect to the incident wave is disturbed greatly, because of the time of travel in the thin plate. Schoch (53) (54) (55) has investigated the transmission of sound through thin plates and shows many pictures of the displacement of reflected sound waves, the non-specular reflection of a beam into smaller beams at various angles, and also shows sound being emitted from the ends of such plates suspended at one end as evidence of the wave-guide effect.

Figures 23 (a) and (b) were taken at  $49^{\circ}30'$  and at  $60^{\circ}$  to ascertain if there were evidence present for discounting the ill-fitting points on the graph. Both show a displacement of the reflected beam, which is characteristic for the excitation of Rayleigh surface waves in the plate.

That there are some good points in this region can be explained by the fact that the three trials were taken on different days, and that the temperature of the liquids was not the same each day. Therefore the angle, which is suitable for matching velocities of the Rayleigh waves and of the trace points parallel to the reflector, would be different according to the temperature.



a. Incident Angle  $49^{\circ} 30'$ .



b. Incident Angle  $60^{\circ}$ .

Figure 23. Evidence of Rayleigh Waves in Mica Film.

### Diffraction Field Before A Long Narrow Quartz

The photograph shown in Figure 24 is an enlargement of the diffraction field near a one-inch long,  $71^\circ$  x-cut quartz, which was excited at 4.42 mc/sec. The width of the quartz was 2.49 mm; excited in carbon-tetrachloride which was chosen because of its low velocity, 940 m/sec, the wavelength was small,  $\lambda = .213$  mm, and the ratio of D to  $\lambda$  became 11.56.

Figures 6 and 7 give the geometrical drawings for the diffraction patterns which are expected from this ratio for the cases of zero and  $\pi$  phase difference between the two cylindrical waves emergent from the edges of the quartz and the plane progressive waves produced by the piston-like action of the special quartz cut.

The agreement between the enlarged field in Figure 24 and the drawing for the  $\pi$  phase difference between the waves is very good in the triangular region marked on Figure 7. Also the directions of the walls of the beam lobes going away from the quartz is in better agreement with the same drawing than it is with that for zero phase difference.

Perhaps it is possible to obtain photographs with sharper interference points and wave fronts but the principal difficulty lies in heat-schlieren at the surface of the transducer. This effect is especially noticeable in  $\text{CCl}_4$ , and the shorter exposure obtained with brighter illumination was used at a sacrifice to longer duration of the light and a more diffuse pattern in the diffraction field.

Sketches similar to those of Figures 6 and 7 drawn for  $D = 10.38\lambda$  were compared with a photograph from the paper by Osterhammel. Because

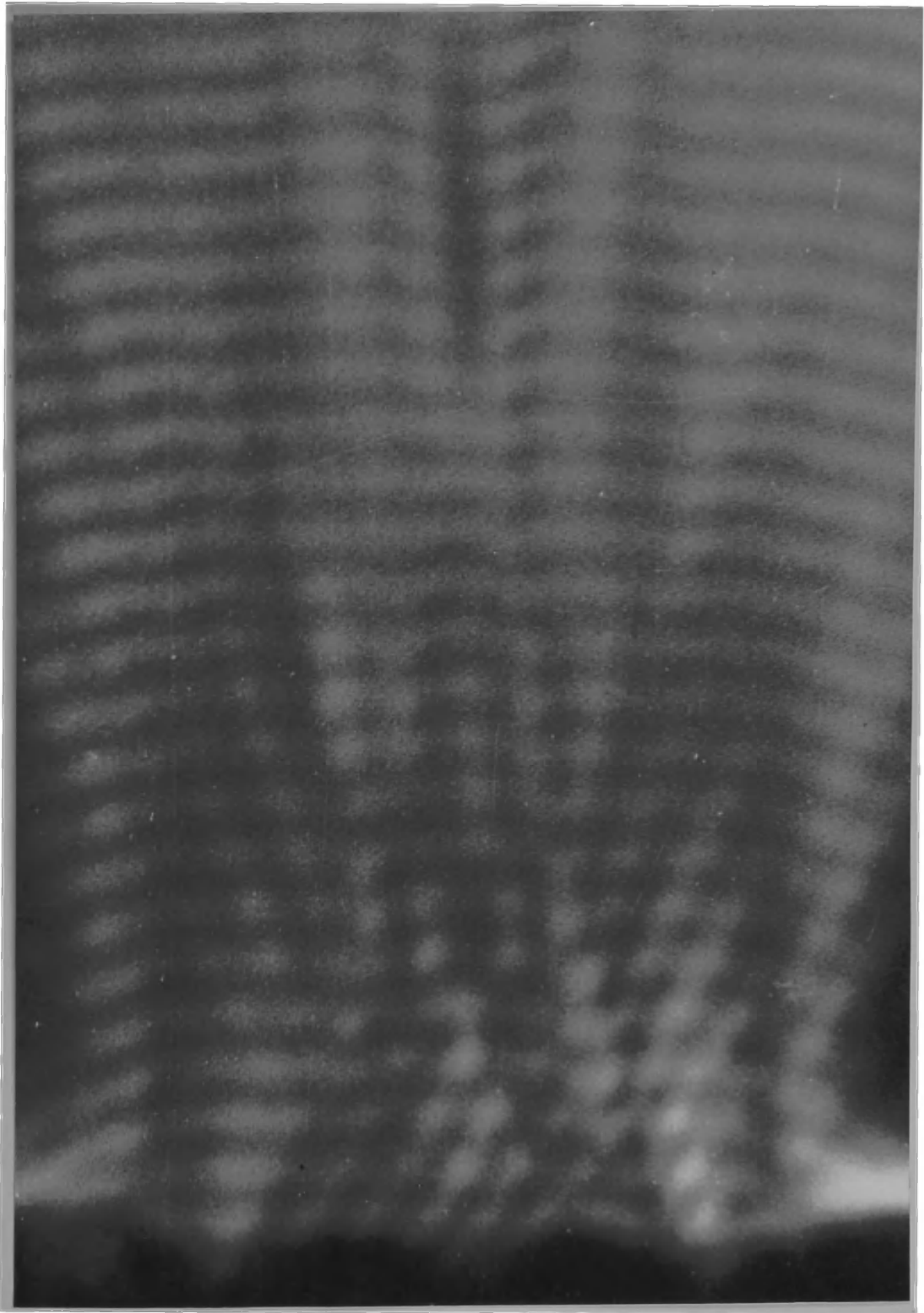


Figure 24. Enlarged Image of the Neighborhood of a Long Thin Quartz.

the photograph is a simple intensity pattern, the side lobes on the drawing were sketched. The angles between the normal to the quartz and the lobe directions were measured and were compared with those on the photograph. The general pattern near the quartz as well as the angles were in best agreement with that drawing for the  $\pi$  phase difference.

## Phase Change at Focus of a Cylindrical Lens

The stroboscopic examination of the sound-field at the focus of a cylindrical lens appears to be a simple matter. Two aluminum lenses were produced by cutting holes of one and one and one-half inches in two one inch thick blocks. The holes were bored on a lathe; the inner surface received a fine mirror finish. The two blocks were then sawed in half to furnish four lenses. The best half of each block was then finish-sanded on the plane surface to remove all scratches. Figure 25 shows the wave-field using the lens with a radius of curvature of one inch. The liquid is xylene and the transducer frequency 2.0 mc/sec. A one inch square quartz transducer was used because it was more simple to select a homogeneous portion of the wavefield from it than from the smaller three-quarter, and one-half inch transducers.

The larger aluminum lens had a focal length which was too long to be used readily within the available light field. Both lenses used were astigmatic so that lead foil had to be folded over the edges of the lens to limit the effective aperture. The opening for sound transmission was reduced by this method to approximately one centimeter width.

Theory predicts that a measurement in the region of the focus of cylindrical lens over a distance greater than seven wave lengths on each side of the focal point will give:  $(n - \frac{\pi}{2})\lambda$ . It is well known that a perfectly formed convergent beam is extremely difficult to obtain experimentally. As it can be seen from Figures 19 and 25 extraneous rays are usually present. A lens focus pattern was sought which would give the best smooth cylindrical curves both before and after the focus. The photograph, Figure 25, from which the measurements were taken had the best curves, free from ripples, but it will be noted that there is a lobe-

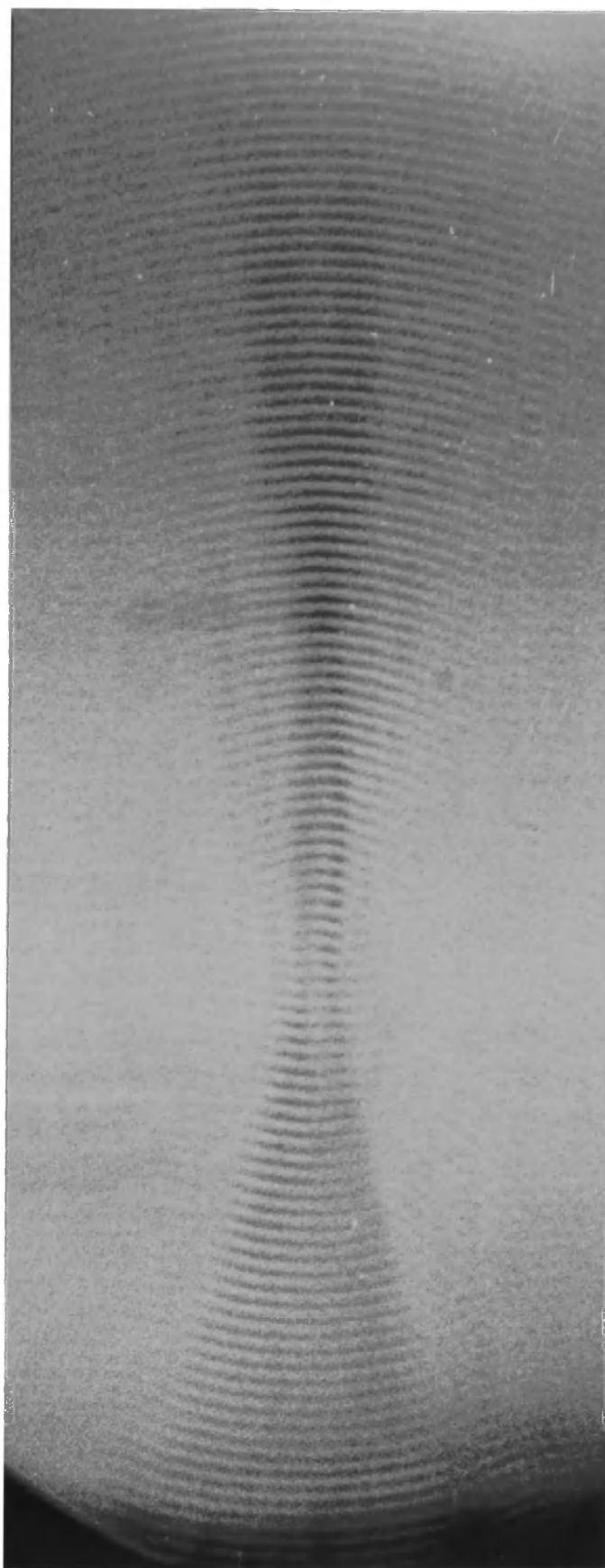


Figure 25. Sound Waves Brought to a Focus by Cylindrical Lens.



like structure after the focus.

A distance of twenty wavelengths was measured to obtain the apparent wavelength  $\lambda'$  of sound; the real wavelength is of no importance because only the added portion of a wavelength which will be introduced is of interest. To avoid errors arising from structure near the focus, it was necessary to make the measurements for  $\lambda'$  in the most distant region from the focus; the measurements of each distance were taken and a simple average used.

The results obtained from a large number of trials on the same film were varied. Theory predicts that the distance over sixty spaces on the photograph be  $\lambda/4$  shorter than sixty wavelengths. Although a few trials suggested that there was a shift of approximately  $3\pi/4$ , the majority was grouped about a shift of  $\pi/2$  which is the predicted result for a spherical lens.

The region near the focus was examined in the following manner. By studying the curvature of the wavefronts in the focal region a central wave was chosen. Twenty individual comparator settings were made on this line and twenty on the fifteenth wavefront before this central line. Readings which differed by more than twice the mean deviation were discarded. Then this distance was compared with a distance equal to fifteen times the wavelength it was found to be larger by an amount equal to  $0.72 (2\pi)$ , or  $\approx 3\pi/2$ . This would mean a phase retardation rather than a phase advance as predicted by Reiche.

Thus none of the measurements gives a result close to the  $\pi/2$  value which is predicted.

There are two obvious sources of error present. The first is that due to diffraction effects throughout the field and especially in the

region of the focus. The second source is the line width which is approximately equal to  $\lambda/2$ . A large number of settings were used to approximately equal to  $\lambda/2$ , moving the hairline of the comparator at the center of the wavefront; but it is readily recognized that the eye is susceptible to psychological suggestion, more so because of the necessity of always bringing the hairline up to the center from one direction.

Further work can be done on this method before it is completely abandoned. It is suggested that an alcohol-water mixture be used as the liquid medium in order to obtain a zero temperature-coefficient for the velocity at the focus where there is an extremely great energy concentration.

## CONCLUSION

The use of Bär's stroboscope is especially well suited for the illumination of large sound fields with greater light intensity than can be expected from previous stroboscopes at high frequencies. The method covers the frequency range from at least 100 kc/sec to approximately 20 mc/sec.

The basic limitation of the method is that all parts of the field cannot be illuminated with the same intensity and the same duration of light. But, if only a small field is desired, one may select that portion of the field which will furnish light of satisfactory duration. If very large intensities are desired more than a short duration of light, the optical arrangements, shown in Figure 16, where no image at slit  $S_2$  is used, will serve the best.

The direction of propagation of the action in  $T_2$  is not dependant upon the orientation of the sound in  $T_1$ , and the motion in  $T_2$  can be of any type of repetitive process. The use of a source slit  $S_1$  requires that the sound in  $T_1$  be perpendicular to the slit, the bending of the light at  $D'$  would vary along the length of the slit, and the phase of the stroboscopic action over the field would not be the same, nor would the duration of light be as small as possible for the total light intensity. This ceases to be a factor when a circular aperture is used as the source.

Once the optical arrangements were ~~once~~ adjusted, no further care was required to keep the unit functioning for long periods of time.

# BIBLIOGRAPHY

1. R. Bar, *Helv. Phys. Acta* (8), 9, 654, 678 (1936).
2. J. C. Maxwell, *Proc. Royal Soc.*, (A) 22, 46 (1876).
3. R. Lucas, *Revue D'Acoust.*, 8, 121 (1939).
4. R. Lucas, *C. R. Acad. Sci, Paris*, 206, 827 (1938).
5. R. Lucas, *J. Physique et Rad.*, (7) 10, 151 (1939).
6. A. Peterlin, *Zbornik dr. Ljubljana*, 2, 24 (1941).
7. A. Peterlin and H. A. Stuart, *Z. Physik*, 112, 1 (1939).
8. S. Oka, *Kolloid Z.*, 87, 37 (1939).
9. S. Oka, *Z. Physik*, 116, 632 (1940).
10. R. Pohlmann, *Z. Physik*, 107, 497 (1937).
11. L. V. King, *Proc. Royal Soc., Lond.*, (A) 153, 17 (1935).
12. V. Zvetkow, A. Mindlina, and G. Makarov, *Acta Physicochimica U.R.S.S.*, 21, 135 (1946).
13. G. Bennett and D. Hall, *J. Amer. Acoust. Soc.*, 25, 1014 (1953).
14. W. Cady, Technical Report No. 7, Scott Laboratory of Physics, Middletown, Conn., 19 (Mar. 20, 1950).
15. D. A. Hall, Master's Thesis, Mich. State College (1954) pp. 14.
16. C. Sadron, *J. Phys. et Rad.*, 7, 263 (1936).
17. A. Peterlin and H. A. Stuart, Doppelbrechung Insbesondere Künstliche Doppelbrechung, *Hand- und Jahrbuch der Chemischen Physik*, Band 8, Abschnitt IB, 44, 54, 56 (1943).
18. G. Goudet, La Modulation de la Lumiere en Haute Frequence par les Ondes Stationnaires Ultra-Sonores; Masson, Paris (1942).
19. E. A. Hiedemann, *Ergebn. der Exact. Naturwiss.*, 14, 214 (1935).
20. P. Debye and F. W. Sears, *Proc. Nat. Acad. Sci., Wash.*, 18, 409 (1932).
21. R. Lucas and P. Biquard, *C. R. Acad. Sci., Paris*, 194, 2132 (1932).

22. C. V. Raman and N. S. N. Nath, Proc. Indian Acad. Sci., A, 2, 406 (1935).
23. K. Grant, Nature, Lond., 120, 586 (1927).
24. F. Duschinsky, Zeits. f. Phys., 81, 7, 23 (1933).
25. E. Hiedemann and K. Hoesch, Zeits. f. Phys., 102, 253 (1936).
26. E. Hiedemann and K. Hoesch, Zeits. f. Phys., 96, 268 (1935).
27. O. Maercks, Zeits. f. Phys., 109, 685 (1938).
28. G. Goudet, C. R. Acad. Sci., Paris, 214, 742 (1942).
29. K. L. Rau, Optik, 5, 277 (1949).
30. R. Tawil, C. R. Acad. Sci., Paris, 191, 92, 998 (1930).
31. P. Cermak and H. Schoeneck, Ann. der Phys., 26, 465 (1936).
32. F. E. Fox and G. D. Rock, Rev. Sci. Instr., 10, 345 (1939).
33. A. Giacomini, Ric. Scient., 17, 900 (1947).
34. Lord Rayleigh, The Theory of Sound, Second Edition, Macmillan (1896), Vol. II, pp. 84 (Reprinted 1929).
35. A. Arons and D. Yennie, J. Acoust. Soc. Amer., 22, 231 (1950).
36. C. Bachem and E. Hiedemann, Zeits. f. Phys., 91, 418 (1934).
37. T. Young, Phil. Trans., Lond., 12, 387 (1802).
38. A. Sommerfeld, Math. Ann., 47, 317 (1896).
39. K. Schwarzschild, Math. Ann., 55, 177 (1902).
40. K. Osterhammel, Akust. Zeits., 6, 6 (1941).
41. L. G. Gouy, C. R. Acad. Sci., Paris., 110, 1251 (1890).
42. F. Reiche, Ann der Phys., (4), 29, 65 (1909).
43. Radio Amateur's Handbook, 26th Edition, Amer. Radio Relay League, West Hartford, Conn., (1949) pp. 194, 198, 200.
44. O. Nomoto, T. Kishimoto and T. Ikeda, Bull. Kobayasi Inst. Phys. Res., 2, 72 (1952).
45. O. Maercks, Phys. Zeits., 37, 562 (1936).
46. R. Lucas and P. Biquard, J. Phys. Radium, 3, 464 (1932).

47. J. Kolb and A. P. Loeber, J. Acoust. Soc. Amer., 26, 249 (1954).
48. A. P. Loeber and E. A. Hiedemann, J. Acoust. Soc. Amer., 26, 257 (1954).
49. O. Wiener, Ann. der Physik (3F), 49, 105 (1893).
50. A. P. Loeber, Ph. D. Thesis, Mich. State College, (1954).
51. L. Cremer, Akust. Zeits., 7, 81 (1942).
52. J. Götz, Akust. Zeits., 8, 145 (1943).
53. A. Schoch, Acustica, 2, 1 (1952).
54. A. Schoch, Acustica, 2, 18 (1952).
55. A. Schoch, Il Nuovo Cimento (9), 7, 1 (1950).